HANNA, LEWIS S.

NICOTINATE PHOSPHORIBOSYL TRANSFERASE FROM YEAST: A NEW HIGH PRESSURE LIQUID CHROMATOGRAPHY ASSAY PROCEDURE, A NEW PURIFICATION PROCEDURE AND A KINETIC ANALYSIS

City University of New York PH.D. 1981

Nicotinate Phosphoribosyltransferase from Yeast: A New High Pressure Liquid Chromatography Assay Procedure, A New Purification Procedure and A Kinetic Analysis.

by

Lewis S. Hanna

A dissertation submitted to the Graduate Faculty in Biochemistry in partial fulfillment of the requirements for the degree of Doctor of Philosophy, The City University of New York

1981

This manuscript has been read and accepted for the Graduate Faculty in Biochemistry in satisfaction of the dissertation requirement for the degree of Doctor of Philosophy.

6
8/17/81
Date

Chairman of Examining Committee

July 16, 1981
Date

Executive Officer

Supervisory Committee

ABSTRACT

Nicotinate Phosphoribosyltransferase From Yeast:
A New High Pressure Liquid Chromatography Assay Procedure,
A New Purification Procedure and A Kinetic Analysis.

by

Lewis S. Hanna

Adviser: Dr. Donald L. Sloan

Nicotinate phosphoribosyltransferase (N_aPRTase) catalyzes the formation of nicotinate mononucleotide (N_aMN) from phosphoribosyl-α-pyrophosphate (PRPP) and nicotinic acid (N_A). The enzyme from several sources hydrolyzes 1 mole of ATP to ADP and inorganic phosphate for every 1 mole of N_aMN formed. This thesis describes the development of a highly sensitive, reliable and fast assay procedure, utilizing high pressure liquid chromatography (HPLC), for N_aPRTase from baker's yeast. The concomitant utilization of the substrates ATP and N_A is followed as is the formation of the products ADP and N_aMN. The assay procedure enabled me to demonstrate the 1:1 stoichiometry between the hyrolysis of ATP and the formaton of N_aMN. Moreover, it enabled me to investigate the kinetics of the N_aPRTase catalyzed reaction faster and with greater accuracy than the previously published procedure which made use of radioactive nicotinic acid.

A purification procedure which provided a very good yield of purified enzyme has been developed employing Phosphocellulose, Hydroxylapatite, Blue-Sepharose CL-6B and DEAE-cellulose chromatographic steps. The procedure produced a 5% yield (10 mg per 6 pounds of yeast) of enzyme with a specific activity of 4.4 units per mg (1 unit = umole of N_aMN formed per min). The molecular weight was determined to be 45,000 by SDS-gel electrophoresis.

Kinetic analysis of the $N_aPRTase$-catalyzed reaction yielded the following results. Utilizing the HPLC assay procedure, double reciprocal initial velocity plots were constructed using data obtained by varying one substrate at different concentrations of the second substrate while maintaining the third substrate constant (6 families of plots) and by varying one substrate at different concentrations of the other two substrates which were maintained at a constant ratio (3 families of plots). In addition, product inhibition studies, with the product pyrophosphate, was performed: 1) at various concentrations of ATP and unsaturated and saturated conditions of N_A, 2) at various concentrations of N_A and unsaturated and saturated conditions of ATP and 3) at various concentrations of PRPP at saturated conditions of N_A. During these studies I observed a significant substrate inhibition at high concentrations of PRPP. In addition I demonstrated that purified $N_aPRTase$ possesses an ATPase activity only in the presence of either product (pyrophosphate or N_aMN) and in the absence of PRPP. Exchange studies between $[^{14}C]$-N_A/N_aMN in the presence and absence of ATP and PRPP and exchange studies between $[^{32}P]$-PP_i/PRPP in the presence and absence of ATP and N_A were accomplished. Binding studies of $[^{14}C]$-N_A to $N_aPRTase$ were also performed in the presence and absence

of ATP and PRPP, and effects of $Cr^{III}ATP$ and $Cr^{III}PP_i$ on the N_aPRTase-catalyzed reaction were initiated. $Cr^{III}ATP$ was observed to be a competitive inhibitor of Mg-ATP function whereas $Cr^{III}PP_i$ and the product $MgPP_i$ inhibited the N_aPRTase activity differently.

All of the above kinetic studies implicate a Uni Uni Bi Ter Ter Quad Ping-Pong system, in which the second and third products dissociate at random, as the kinetic mechanism for the N_aPRTase reaction. The K_m values for ATP, PRPP and N_A were calculated to be 70±10 uM, 24±3 uM and 23±4 uM respectively, whereas a V_{max} value of $2.5\pm0.4 \times 10^{-2}$ umol N_aMN/min and a value for $K_{i(PRPP)}$ of 5±1 uM were determined.

ACKNOWLEDGEMENTS

This thesis is dedicated to my father and my wife whose love, patience and encouragement have helped to bring this thesis to its successful completion.

I would like to thank the members of my thesis committe, Dr. Sharon Cosloy, Dr. Morton Glantz, Dr. Thomas Haines and Dr. William Sweeney for their cooperation and valuable advice.

I would also like to thank Susan Hess for her great help in the purification procedure and making great coffee, Danyel Syed for his help in the Cr^{III}-complex syntheses, and Linda Ali and Robert Ashton for their valuable suggestions.

Finally, I would like to greatly thank my mentor, Dr. Donald Sloan for the patience, support and encouragement he has generously shown during this work.

TABLE OF CONTENTS

LIST OF TABLES

LIST OF FIGURES

INTRODUCTION

Nicotinamide adenine dinucleotide (NAD) can be synthesized by three different pathways in living cells (Fig. 1).

In the de-novo pathway tryptophan is metabolized to either or both nicotinic acid (N_A) and quinolinic acid (Q_A). Quinolinate phosphoribosyltransferase, QPRTase, (Nicotinatenucleotide:pyrophosphate phosphoribosyltransferase (carboxylating), EC. 2. 4. 2. 19)[1] then catalyzes the decarboxylation of quinolinic acid at the 2-position and the formation of a β-glycosidic bond between the base and the ribose-5'-phosphate moiety of 5'-phosphoribosyl-1'-pyrophosphate (PRPP), to produce nicotinate mononucleotide (N_aMN). N_aMN can also be synthesized from nicotinic acid (Preiss - Handler pathway)[2] through the action of nicotinate phosphoribosyltransferase, N_aPRTase, (Nicotinatenucleotide:pyrophosphate phosphoribosyltransferase, EC. 2.4. 2. 11), where nicotinic acid is obtained either from nutritional sources or from tryptophan metabolism. NAD can be synthesized from N_aMN in two steps, the addition of the AMP portion of NAD followed by the formation of the amide group.[3,4] In the third route, nicotinamide can serve as precursor for the formation of nicotinamide mononucleotide (NMN) through the action of nicotinamide phosphoribosyl transferase, (Nictotinamidenucleotide:pyrophosphate phosphoribosyltransferase, EC. 2. 4. 2. 12).[5] Thereafter NAD is synthesized directly through the addition of the AMP portion.

It appears that there is more than a single pathway for NAD synthesis in any single organism.[6-8] Nicotinamide can serve as precursor in bacteria[9] and yeast[5] whereas quinolinic acid can serve as precursor in rat,[1] bovine and hog liver,[10, 11] castor

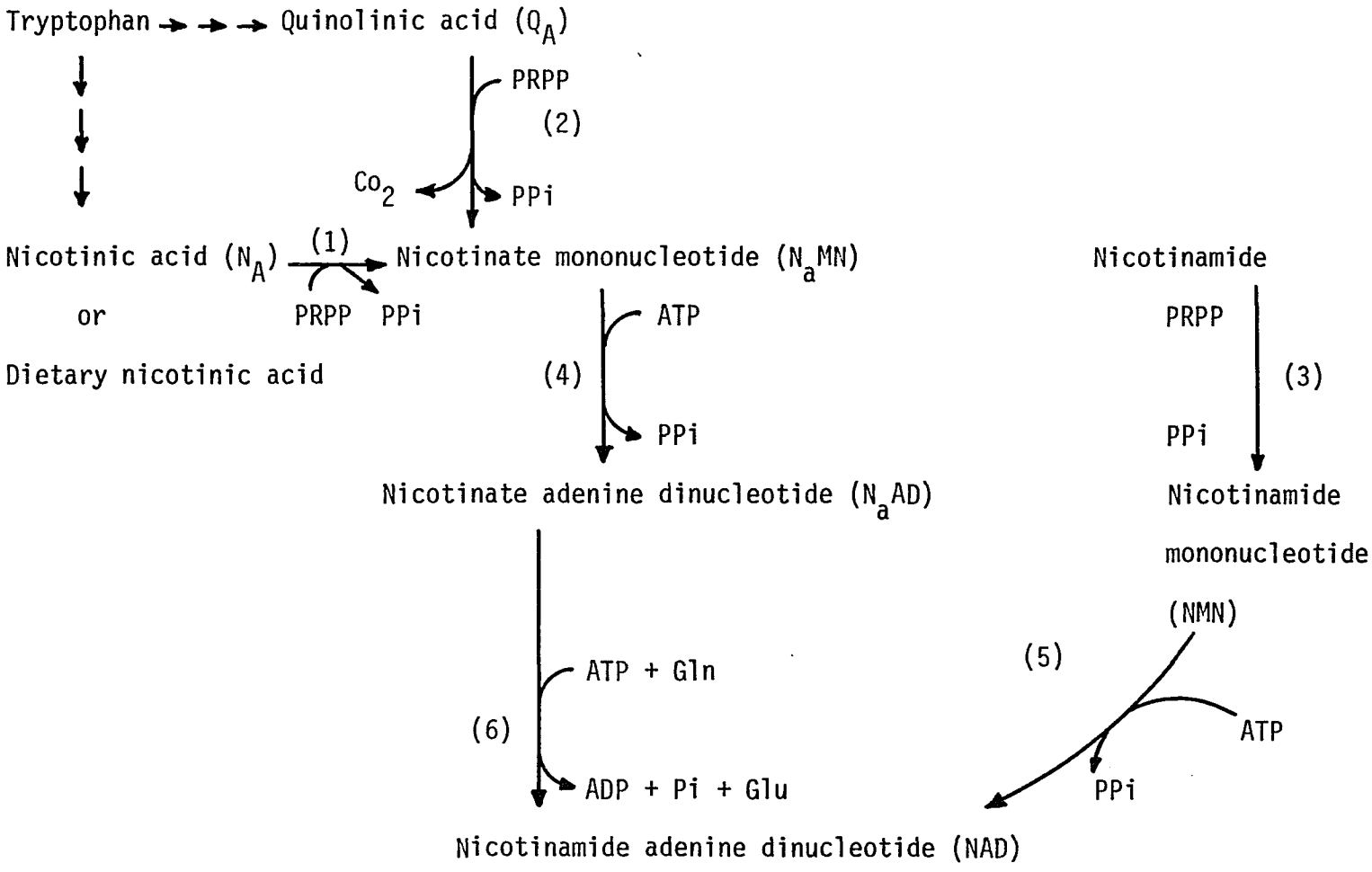

Figure 1. Pathways for NAD synthesis. The enzymes catalyzing different steps are (1) Nicotinate phosphoribosyltransferase, (2) Quinolinate phosphoribosyltransferase, (3) Nicotinamide phosphoribosyltransferase, (4) Nicotinatemononucleotide/adenylyltransferase, (5) Nicotinamidemononucleotide/adenylyltransferase and (6) NAD^+ synthetase.

bean endosperm,[12] "Shiitake" mushroom,[13] pseudomonad[14] and Alcaligenes eutrophus nov. subsp. quinolinicus (A.E. quinolinicus).[15] However, the main route for the biosynthesis of NAD in mammalian tissue, yeast and E. coli is the Preiss-Handler pathway. Moreover, it has been suggested that different precursors serve as the primary source of NAD under different cellular growth conditions in E. coli.[16]

The above-described phosphoribosyltransferases share the cellular PRPP with other purine and pyrimidine phosphoribosyltransferases. The allocation of PRPP to this group of enzymes depends on its availability as well as the turnover rate, stability and rate of synthesis of every enzyme, in addition to the effect of the products and allosteric effectors on the reaction rates.[17] Any malfunction in this stringent regulatory system can cause severe disorders in man. For example, hyperuricemia (the excessive production of uric acid) is the result of an increase in PRPP amidotransferase activity (the first step in the de-novo purine biosynthesis).[18, 19] Lesch-Nyhan syndrome is the result of a complete deficiency in hypoxanthine-guanine phosphoribosyltransferase (HGPRTase), the enzyme catalyzing the formation of inosine-5'-monophosphate (IMP) and guanosine-5'-monophosphate (GMP).[20] Another metabolic disorder associated to the phosphoribosyltransferases is orotic aciduria which is the result of a complete deficiency in orotate phosphoribosyltransferase (OPRTase), the enzyme catalyzing the formation of orotidine-5'-monophosphate (OMP).[21] Gershon and Fox[22] have observed that administration of megadoses of nicotinic acid produced hyperuricemia without increasing the uric acid concentration in urine. This may suggest an interrelation between the purine nucleotide and pyridine nucleotide bio-

synthetic pathways, which needs to be investigated further.

1. Nicotinate Phosphoribosyltransferase (N_aPRTase)

Nicotinate phosphoribosyltransferase (N_aPRTase) catalyzes the first step in Preiss-Handler pathway for the biosynthesis of NAD, producing N_aMN from PRPP and nicotinic acid. N_aPRTases isolated from different sources[4, 23-29] have an absolute requirement for a divalent metal ion and catalyze the formation of N_aMN irreversibly. Moreover, phosphate ion seems to stimulate N_aPRTase activity. However, molecular weights and nucleotide requirements differ depending on the source of the enzyme. For example, the bovine liver N_aPRTase[23] has a molecular weight of 86,000 which is twice that for the yeast enzyme.[24, 25] The yeast, E. coli[4] and B. subtilis[26] N_aPRTases require an essential (however nonspecific) nucleotide. In addition to ATP, these enzymes can utilize GTP and ITP and to a lesser extent CTP and UTP. ATP, specifically, is a positive allosteric modifier of the N_aPRTases from bovine liver,[23] human erythrocytes[27] and Ehrlich Ascites tumer cells.[28] Moreover, N_aPRTase from protozoan Astasia longa[29] is ATP independent. The ATP requirement in certain organisms may provide a control system crosslinking energy metabolism and NAD biosynthesis. It has been determined that a 1:1 stoichiometry exists between ATP consumption and the formation of N_aMN in B. subtilis, human erythrocytes and yeast.[24-27]

Because of a time consuming C^{14}- nicotinate to C^{14}- N_aMN assay procedure involving the separation of nicotinate from N_aMN by paper chromatography[24] and because of a lengthy purification procedure with very poor yield,[4, 23-29] little is known about the mechanism

and properties of N_aPRTase from different sources. One of the most studied N_aPRTase is from baker yeast.[24, 25] The enzyme has a broad pH optimum for enzyme activity centered near pH 8.0. Kosaka et al.,[25] have demonstrated that a phosphorylated enzyme is quite likely to be a catalytic intermediate. Moreover, they have suggested two different kinetic mechansims for the action of yeast N_aPRTase. These two mechanisms are defined as a partial ordered substrate binding and/or a partial ping-pong substrate binding with partial random product release.

2. Comparisons Between N_aPRTase and QPRTase

Although N_aPRTase and QPRTase give rise to the same product (N_aMN), they utilize different substrates (nicotinic acid and quinolinic acid respectively). QPRTases purified from hog kidney,[30] hog liver[31] and A.E. quinolinicus[15] all have a molecular weight of about 210,000 and are composed of 6 identical subunits of 34,200 M.W., whereas N_aPRTase purified from yeast consists of a single polypeptide chain of about 45,000 M.W.[24] and N_aPRTase purified from beef liver has a molecular weight of 86,000.[27] Like N_aPRTase, QPRTase has an absolute requirement for a divalent metal ion and displays maximal activity in the presence of phosphate ion. The exception to this is QPRTase from A.E. quinolinicus which is inhibited by phosphate ion. The pH optimum for QPRTase from different sources ranged from 6.1-9.5, whereas N_aPRTases have pH optima of 7-8.5 independent of the enzyme source. QPRTase from A.E. quinolinicus displays maximal activity at 60°C, whereas N_aPRTases from different sources are heat labile. Moreover,

nucleoside triphosphates serve either as substrates (yeast) or as positive allosteric modifiers (beef liver) for N_aPRTase activity, whereas these nucleotides inhibit QPRTase from different sources.[15,30,31] Diphosphate nucleotides are inhibitors for N_aPRTases that require a triphosphate nucleotide, whereas they have no inhibitory effect on QPRTase activity. Nucleoside monophosphates as well as ribose-1-phosphate (R-1-P) and ribose-5-phosphate (R-5-P) have no inhibitory effect on either N_aPRTases or QPRTases from any source. Amino acid modifiers were employed to determine that QPRTAase from hog liver,[31] hog kidney[30] and A.E. quinolinicus[32] contain lysine, histidine and cysteine at their active sites. Such studies have not been conducted for N_aPRTase. Double reciprocal plots of the initial rate of N_aMN formation vs. substrate concentrations for QPRTase from hog liver[31] and hog kidney[33] are composed of sets of parallel lines indicative of ping-pong kinetic mechanisms, whereas these plots for QPRTase from A.E. quinolinicus[34] are composed of intersecting lines indicating that this enzyme proceeds through the use of a sequential mechanism. Thus QPRTases from different sources may catalyze their reaction through different kinetic mechanisms.

3. Mechanisms of Action of Other PRTases

Different PRTases from different sources show a wide range in molecular weight, K_m values for PRPP and K_m values for the nitrogenous substrates. These differences exist for the same PRTase enzyme from different sources and for different PRTases from the same source. Moreover, different PRTases catalyze their reaction through different

kinetic mechanisms. For example, earlier studies on HGPRTase from human erythrocytes[35] suggested a ping-pong Bi Bi kinetic mechanism because of the appropriate parallel double-reciprocal initial velocity lines were obtained and because of an initial burst of IMP synthesis upon the addition of hypoxanthine to an enzyme preincubated with and purified from PRPP and Mg^{2+} was also observed. However, later studies[36] indicated that the HGPRTase catalyzed the reaction through an ordered bibi mechanism in which the products IMP and pyrophosphate (PPi) were released from the enzyme by rapid equilibrium random dissociation. Henderson et al.[37] interpreted the initial velocity patterns by proposing that K_{iA} is much smaller than K_{mA} which would result in an apparant parallel pattern of lines, whereas the ordered mechanism is, in fact, functioning. Papaioannou and his colleagues,[38] later showed that the ratio of K_{iA} to K_{mA} was greater than 0.1 and that intersecting lines should be observed. Furthermore, they proposed that, at an optimum metal ion concentration, a ping-pong mechansim is in effect whereas ordered mechanism is in effect at low concentration of metal ion. Giacomello and Salerno[36] have disagreed with this proposal and the question is still unresolved.

It has been observed by Victor et al.[39] that OPRTase from baker yeast catalyzes the formation of OMP through a ping-pong Bi Bi kinetic mechanism at optimal metal ion concentrations. Double reciprocal initial velocity analysis, product inhibition studies and exchange studies between radioactive substrate/product pairs led to this conclusion.

ATP-PRTase from Salmonella typhimurium proceeds through the use of an ordered kinetic mechansim as determined by kinetic analysis,[40-43] even though earlier studies[44] had suggested a ping-pong mechanism because of the apparent isolation of a labelled phosphoribosylated enzyme intermediate.

Generally, ping-pong mechanisms in a Bi Bi reaction system will define a double displacement mechanism which usually leads to retention of configuration, whereas PRTases catalyze an inversion of the glycosidic bond configuration.[41, 45] This has been the main objection to a ping-pong mechanism as the mechanism of action for some PRTases. An S_N2 mechanism, based on stereochemical consideration only, has been proposed for OPRTase.[46] One has to keep in mind that for those PRTases with a suggested ping-pong kinetic mechanism, a more complicated mechanism than double displacement must be proposed. Formation of a carbonium ion intermediate as the mechanism by which yeast OPRTase proceeds has been proposed by Parsons and colleagues.[47]

4. Rationale

Work in this laboratory has been directed toward the purification and characterization of several PRTase enzymes from a single source (yeast), so that a comparison can be made of their properties.[48-50] Out of this work should come a delineation of how PRPP is allocated among the various biosynthetic pathways in this organism. The present work describes our purification and characterization of N_aPRTase from yeast which has been facillitated with design of a new HPLC assay for this enzymatic activity. Because our assay procedure is fast and very

sensitive, we wished to showcase its potential by accomplishing a detailed kinetic analysis of the N_aPRTase catalyzed reaction.

In this thesis I present: a) initial velocity determinations over a range of ATP, PRPP and nicotinate concentrations, b) initial velocity determinations of the ATPase activity that this enzyme displays under certain conditions, and c) the inhibition of N_aPRTase activity by newly synthesized Cr^{III}ATP and Cr^{III}PPi. All of this work sets the stage for NMR studies of the N_aPRTase-catalyzed reaction.

MATERIALS

Pressed baker's yeast (Budweiser brand) was obtained from Valenti Yeast, Inc., Flushing, New York. ATP (disodium salt), ADP (sodium salt), AMP (sodium salt), nicotinic acid, N_aMN (acid form) and PRPP (sodium salt) were purchased from Sigma Chemical Company, St. Louis, MO. Ammonium phosphate, potassium phosphate (mono- and di-basic salts) were purchased from Fisher whereas sodium pyrophosphate was a Baker Analytical reagent. Orotic acid was purchased from Calbiochem., Inc., La Jolla, CA. Phosphocellulose was purchased from Brown Company, Berlin, N.H. Hydroxylapatite HT, DEAE-cellulose (Cellex D.) and Dowex AG-1-X8 anion exchange resin (formate form) were purchased from Bio-Rad Laboratories, (Richmond, CA.) whereas Blue-Sepharose CL-6B was purchased from Pharmacia Chemicals, Piscataway, N.J. 7-[^{14}C]-nicotinic acid (free acid) and [^{32}P]-pyrophosphate (sodium salt) were obtained from New England Nuclear, Boston, MA. The reagents for polyacrylamide gel electrophoresis and SDS gel electrophoresis including protein standards were purchased from Bio-Rad Laboratories. All other materials were analytical grade.

METHODS

Radioactive Assay

The activity of N_aPRTase was monitored initially by following the formation of [^{14}C]-N_aMN from [^{14}C]-nicotinate.[24] The reaction mixture contained 0.1 mM 7-[^{14}C]-nicotinic acid (1.0 uCi), 1.0 mM ATP, 0.5 mM PRPP, 5.0 mM $MgCl_2$ and 50.0 mM Tris-phosphate buffer at pH 8.0. The reaction was initiated by the addition of approximately 0.1 milli-unit of the enzyme and was terminated (after incubation for 15 minutes at 37°C) by heating in boiling water bath for 2 minutes. The denatured protein was removed by centrifugation and 25 u1 of the reaction mixture was applied to 1.5 x 13.0 inch strips of Whatman #1 filter paper. The separation of [^{14}C]-nicotinate from [^{14}C]-N_aMN was achieved by descending chromatography in 95% ethanol-1M ammonium acetate pH 5.0 (7:3 v/v) for 5 hours. The paper strip was cut into 2 cm strips, in the direction of solvent flow, and the radioactivity was counted by placing it in vials with 4.0 ml scintilation fluid (toluene-ethanol-omnifluor 3:2:0.025 v/v/w) and counted by a Nuclear-Chicago scintillation counter. N_aMN will migrate shorter distances (stays near the origin) than nicotinate (migrates near the solvent front).

High Pressure Liquid Chromatography (HPLC) Assay

A Waters Associates HPLC instrument equipped with a model 6000 A solvent delivery system, model U6K sample injector, model 440 absorbance detector, and a Houston Omniscribe chart recorder was employed. A single 4 mm x 30 cm u-Bondapack C_{18} column (equilibrated with 25.0 mM $(NH_4)_3$ PO_4 at the appropriate pH and stored in 100% methanol when not

in use) was placed on line with the solvent delivery system. Sample volumes of 5 ul were injected onto the column using a Hamilton 801 microliter syringe. These samples were eluted using a solvent flow rate of 0.7 ml/min (700-1000 psi). Nucleotides and/or bases in the eluent were detected at 254 nm (0.1 -0.01 scale settings).[51-52]

The standard N_aPRTase assay mixture which was injected onto the C_{18} column contained 5.0 mM $MgCl_2$, 0.1 mM nicotinate, 0.1 mM ATP and 0.1 mM PRPP in 50.0 mM Tris-phosphate buffer at pH 8.0. The reaction was initiated with the addition of approximately 0.1 milliunit of enzyme and was terminated (after incubation for 15 min at 37°C) by heating in a boiling water bath for 2 minutes. The samples were then clarified, first by centrifugation and then by passage through a 0.45 micron HA-type Millipore filter. Volumes of 5.0 ul of these samples were then injected onto the column.

During the kinetic analysis, various concentrations of ATP, PRPP, nicotinic acid and pyrophosphate were employed. These concentrations are described in the appropriate figure legends.

Purification of Nicotinate Phosphoribosyl Transferase from Baker's Yeast

Step 1. Autolysis procedure: Forty eight pounds of pressed baker's yeast were suspended in a mixture of 14.4 liters of 0.3 M potassium phosphate buffer at pH 8.0 and 2.4 liters of toluene and gently stirred for 4 hours at 30°C in a constant temperature bath. The pH was maintained at 8.0 by the periodic addition of 5N KOH solution. The suspension was centrifuged in a Sorvall RC-2B refrigerated centrifuge for 20 minutes at 13,000 x g (10,000 rpm) at 4°C. The supernatant

was filtered through glass wool to remove fluffy lipid material mixed with toluene. All steps hereafter described were performed in a cold room maintained at 4°C, except where otherwise specified.

Step 2. Ammonium sulfate fractionation: The autolysate (24.0 l) was adjusted to pH 5.0 with 8 N acetic acid with stirring in the presence of 2-3 ml octanol (an antifoaming agent). The acidified autolysate was brought slowly to 50% saturation with ammonium sulfate (313 g ammonium sulfate/liter). The solution was allowed to stand overnight to effect complete precipitation. The precipitate was collected by centrifugation for 20 minutes at 13,000 x g at 4°C, and redissolved in a minimum volume of 10 mM potassium phosphate buffer at pH 8.0. The solution was adjusted to pH 8.0 and recentrifuged under the same conditions. The solution was then dialyzed overnight against 40.0 l of 10.0 mM potassium phosphate buffer at pH 8.0.

Step 3. Manganese chloride treatment: The dialyzed ammonium sulfate (6.65 l) was brought to 50.0 mM with respect to $MnCl_2$ by the addition of 1.0 M $MnCl_2$ solution to precipitate nucleic acids. The solution was then centrifuged and the precipitate was discarded.

Step 4. Ethanol fractionation: The solution from the $MnCl_2$ treatment (6.50 l) was brought to 0.25 M sodium acetate buffer at pH 6.0 by the addition of 2.0 M sodium acetate buffer at pH 6.0. Solid orotic acid also was added to make the solution 1.0 mM with respect to orotate. These additions were employed to protect orotate phosphoribosyltransferase which can be purified from the same preparation of yeast. The solution was stirred for 30 minutes then cooled to -2°C. To this mixture 95% ethanol (cooled to -20°C by a dry ice-acetone bath) was added

slowly with swirling to a concentration of 50% (temperature was maintained at -10°C by a dry ice-acetone bath). The precipitate was collected immediately by centrifugation at -15°C (speed of 13,000 x g for 20 minutes) and redissolved in a minimum volume of 10.0 mM potassium phosphate buffer at pH 8.0 and the suspension was stirred for 1.0 hour (to a homogenous suspension). This solution was centrifuged and the precipitate was extracted once again with the same buffer and the combined extracts were dialyzed twice for periods of 18.0 hours and 8.0 hours against 20.0 l of 5.0 mM potassium phosphate buffer at pH 6.0. The above purification steps were adapted with some modifications from Umezu et al.[53].

Step 5. Phosphocellulose column chromatography: The dialyzed solution from ethanol fractionation (4.60 l) was layered onto a phosphocellulose column (5.0 x 60.0 cm) pre-equilibrated with 5 mM potassium phosphate buffer at pH 6.0, then washed with the same buffer. The portion of the protein which was not retained on the column, contained the OPRTase activity which could be purified further by the method of Victor et al.[39] N_aPRTase was eluted with 40.0 mM potassium phosphate buffer at pH 6.7. The column was washed with 0.5 M potassium phosphate at pH 6.7 to elute the remainder of the retained proteins. This portion of the eluant did not contain OPRTase or N_aPRTase activity. The fractions containing the N_aPRTase activity were pooled and brought slowly to 70% saturation with solid ammonium sulfate (472 g/liter). The solution was allowed to stand overnight at 4°C and the precipitate was collected by centrifugation for 20 minutes at 13,000 x g at 4°C and redissolved in a minimum volume of 5.0 mM potassium phosphate at pH 7.5. The solution was adjusted to pH 7.5 with 1.0 N KOH solution and dialyzed twice for periods of

8.0 hours and 18.0 hours against 20.0 l of 5.0 mM potassium phosphate buffer at pH 7.5. A typical elution profile for N_aPRTase from phosphocellulose column is illustrated in Figure 2.

Step 6. Hydroxylapatite column chromatography: The dialyzed solution from phosphocellulose column chromatography (165 ml) was brought to 10.0 mM $MgCl_2$, 5.0 mM nicotinate and 2.0 mM PRPP by addition of solid $MgCl_2$, nicotinic acid and PRPP respectively. This was done to change any phosphorylated enzyme to its unphosphorylated form. The solution was allowed to stand at room temperature for 15 minutes. The solution was then cooled and layered onto a hydroxylapatite column (6.0 x 10.0 cm) pre-equilibrated with 5.0 mM potassium phosphate pH 7.5 and washed with the same buffer. N_aPRTase was eluted using a linear gradient (5-100 mM) of potassium phosphate at pH 7.5 followed by 0.5 M potassium phosphate at pH 7.5. The fractions containing the N_aPRTase activity were pooled and brought slowly to 70% saturation with solid ammonium sulfate. The solution was allowed to stand overnight and the precipitate was collected by centrifugation and redissolved in a minimum volume of 2.0 mM Tris/HCl buffer at pH 6.0 and dialyzed for 24 hrs against the same buffer.

Step 7. Blue-Sepharose CL-6B column chromatography: The dialyzed solution was divided into three equal parts of 22.0 ml each and each part was layered onto a Blue-Sepharose CL-6B column (2.5 x 30.0 cm) pre-equilibrated with 2 mM Tris/HCl buffer at pH 6.0, then washed with the same buffer. N_aPRTase was eluted by a linear gradient (2-200 mM) of Tris/HCl buffer at pH 6.0 followed by 0.5 M Tris/HCl buffer at pH 6.0. The fractions containing the N_aPRTase activity were pooled

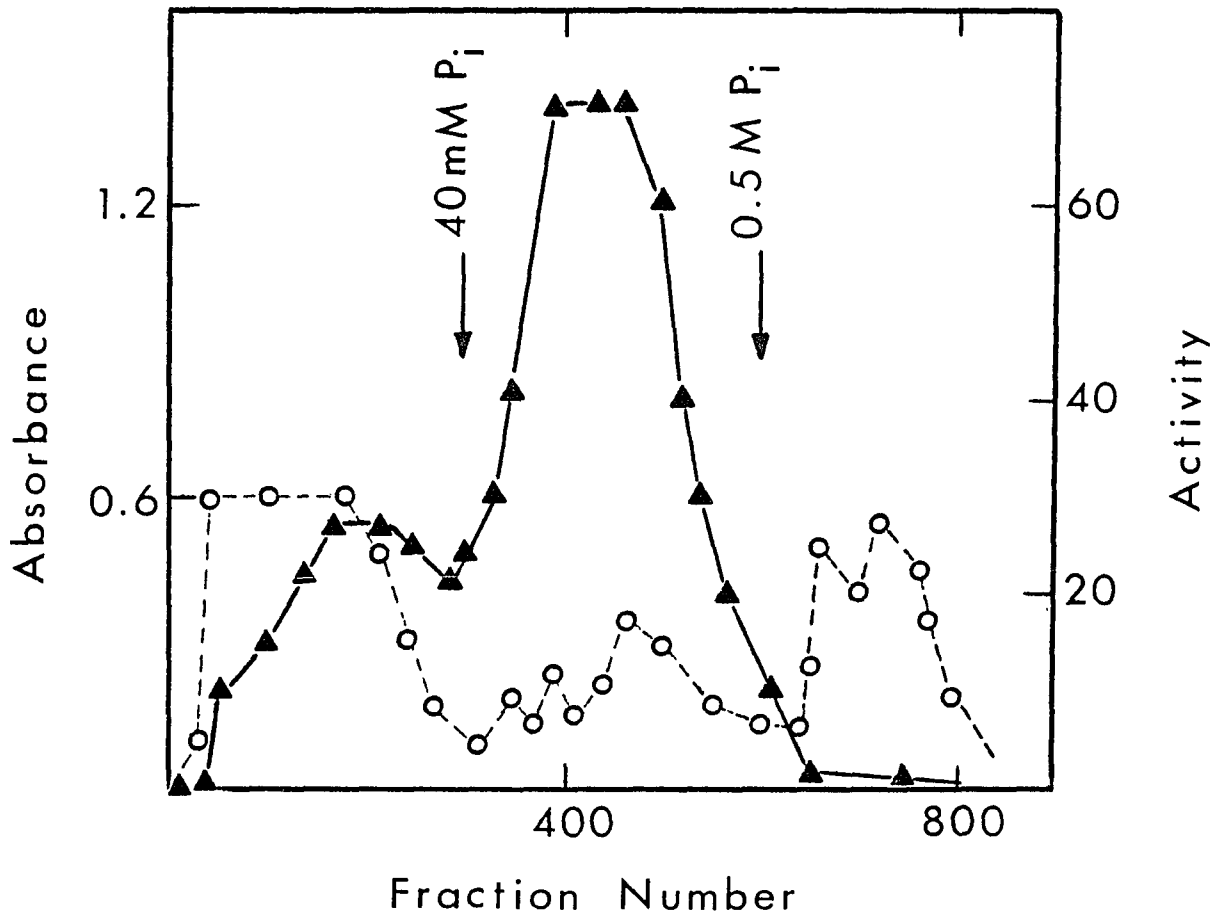

Figure 2. Phosphocellulose elution profile for the purification of N_aPRTase from yeast. The activity of the enzyme (closed triangles) was monitored using the HPLC assay procedure and the units are uM N_aMN formed/min/ml enzyme solution. Protein elution was monitored using the absorbance (280 nm) of each fraction (open circles). Conditions for the run were as described in the "Methods" section.

and lyophilyzed to dryness, then dissolved in a minimum volume of 5.0 mM potassium phosphate buffer at pH 7.5 and dialyzed again for 24 hrs against the same buffer.

Step 8. DEAE-cellulose column chromatography: A pool of the dialyzed fractions from Blue-Sepharose column (37.0 ml) was layered onto a DEAE-celullose column (2.5 x 30.0 cm) pre-equilibrated with 5.0 mM potassium phosphate buffer pH 7.5. N_aPRTase was eluted by a linear gradient (5-100 mM) of potassium phosphate buffer at pH 7.5 followed by a 0.5 M concentration of the same buffer. The fractions containing N_aPRTase activity were pooled and lyophilyzed to dryness and redissolved in a minimum volume of 5.0 mM potassium phosphate buffer at pH 7.5 and dialyzed against 20.0 l of the same buffer for 4.0 hours.

Gel Electrophoresis

Disc gel electrophoresis was performed by the method of Davis[54] utilizing 7.5% polyacrylamide gel preparations at room temperature at pH 8.9. Protein staining was accomplished in 2.0 hours using 1% Coomassie blue solution in 10% acetic acid and 30% methanol. Gels were destained overnight in 10% acetic acid and 30% ethanol solution. Polyacrylamide gel electrophoresis in the presence of sodium dodecyl sulfate (SDS) and in the presence or absence of mercaptoethanol were performed by a modified procedure[55] of Shapiro et al.[56] utilizing the same procedure of staining and destaining mentioned previously. Polyacrylamide gel electrofocusing was performed by the method of Wrigley[57] in cylindrical gels (0.5 x 14 cm) utilizing a Shandon gel electrophoresis apparatus. Gels were immersed in 10% trichloroacetic

acid for 48.0 hours to extract the ampholite which interferes with the staining and destaining processes. The protein will precipitate in white bands which can be seen on a black background. Staining and destaining was accomplished by the method of Reghetti and Drysdale.(58) Staining was performed in 0.05% Coomassie blue and 0.1% copper II sulfate in acetic acid-ethanol-water (10:25:65 v/v/v) overnight, whereas destaining was performed in acetic acid-ethanol-water (10:25:80 v/v/v).

Protein determination

The concentrations of protein in different purification steps were determined by the Lowry procedure.(59)

Isotopic exchange studies

1. Exchange of [^{14}C]-nicotinate into N_aMN: A reaction mixture containing 50.0 mM Tris-phosphate buffer at pH 8.0, 5.0 mM $MgCl_2$, 0.01-0.03 mM [^{14}C]-nicotinate and 1.0 mM N_aMN and approximately 0.1 milliunit enzyme was incubated at 37°C for 15.0 minutes. The reaction was terminated by heating in a boiling water bath for 2.0 minutes. Nicotinate and N_aMN were separated and the radioactivity was counted as described in an earlier section. The above procedure was repeated in the presence of either 0.05 mM PRPP or 0.2 mM ATP and with a control containing no enzyme. The data was represented as % exchange using the equation shown below.

$$\% \text{ exchange} = \frac{\text{number of counts incorporated in } N_a\text{MN} \times 100}{\text{number of counts of } N_a\text{MN} + \text{number of counts of } N_A}$$

2. Exchange of [^{32}P]-pyrophosphate into PRPP: A reaction mixture containing 50.0 mM Tris-phosphate buffer at pH 8.0, 5.0 mM $MgCl_2$, 0.2-0.5 mM [^{32}P]-pyrophosphate, 1.0-3.0 mM PRPP and approximately 0.1 milliunit enzyme was incubated at 37°C for 15.0 minutes. 1.0 ml of 2.5 mM pyrophosphate solution was added at the end of the incubation period and the entire solution was layered on a Dowex AG 1-X8 (ion exchange resin, formate form) column (1.5 x 5.0 cm). PRPP and pyrophosphate were eluted separately by a linear gradient of 0 -1.5 M ammonium formate at pH 5.0 (250.0 ml of each solution). Fractions of 5.0 ml each were collected and 1.0 ml of each fraction was added to 5.0 ml Bray's solution and counted. Pyrophosphate and PRPP were located in the eluant by established methods.[60,61] The above procedure was repeated in the presence of either 1.0-3.0 mM ATP or 4.0 mM nicotinate and with a control containing no enzyme.

Synthesis of Cr^{III} PPi and Cr^{III} ATP

Cr^{III} PPi and Cr^{III} ATP (β,γ bidendate) were synthesized in this laboratory according to Cleland's methods[62-64] in collaboration with Danyel Syed. Total chromium, total phosphate and inorganic phosphate analyses were performed on synthesized Cr^{III} PPi according to established methods.[65-67] The synthesized Cr^{III} PPi showed absorption maxima at 604 and 435 nm and showed 1.0:0.99 Cr:PPi and 98.0% purity. Cr^{III} PPi concentration was determined to be 20.0 mM. The synthesized Cr^{III} ATP showed absorption maxima at 605 ±1 and 425 ±1 nm. Cr^{III} ATP concentration was determined to be 7.5 mM.

Binding Studies with Flow Dialysis

A Technilab (Fisher Scientific) flow dialysis apparatus, first described by Colowick and Womack,[69] was used to study the binding of nicotinate to N_aPRTase. The apparatus consists of two chambers, the upper chamber contains the enzyme and the labelled substrate whereas the lower chamber contains buffer which is pumped through this chamber at a constant rate and then collected in fractions. The two chambers are separated by a membrane, permeable only to the small molecules, and each chamber contains a stirring bar. The assembled apparatus is placed onto a magnetic stirrer.

Concentrations of 20 uM N_aPRTase, 5 mM $MgCl_2$ and 1 mM ATP were incubated for 10 minutes at room temperature, then placed into the upper chamber and after 1 minute 40 uM 7-[^{14}C]-nicotinic acid (0.1 uCi) was added to the upper chamber. The buffer flowing through the lower chamber was 50 mM potassium phosphate (pH 7.4) containing 5 mM $MgCl_2$. The flow rate of 3 ml/min was accomplished using a LKB-2120 Varioperpex II pump and 3 ml fractions were collected. After the collection of five fractions, the following concentrations of unlabelled nicotinate were added to the upper chamber in sequence: 1, 2, 5, 10 and 100 ul of 20 mM nicotinate solution (followed by 100 ul of 0.5 M nicotinic acid). This experiment was repeated in the absence of ATP and in the absence of enzyme, and an additional experiment was run in the presence of 0.5 mM PRPP.

RESULTS

HPLC Assay

Studies of the HPLC elution profiles of a mixture of ATP, ADP, N_aMN and nicotinic acid (Figure 3) suggested that over the pH range of 5-8, N_aMN (3 minutes elution time) can be resolved from the other reactants. However, maximal separation of all the reactants can be achieved using 25.0 mM $(NH_4)_3PO_4$, pH 8.0. I have elected to employ this eluant at pH 8.0 in order to examine how the reaction catalyzed by N_aPRTase proceeds using four measurements, namely, the changes in ATP, ADP, N_aMN and nicotinic acid concentrations with time (vide infra). I am aware, however, that u-Bondapak C_{18} column material is relatively unstable in alkaline solutions. The enzymatic activity is monitored at pH 6.0 and the average of the changes in N_aMN and ATP concentrations with time is used as the measure of activity. Employing known concentrations of the reactants, we have established a direct relationship between the concentrations of the injected substrate and product solutions and the peak heights and peak areas of the resulting elution profile (Figure 4). Peak height measurements and these standard curves were used to calculate the concentration of each reactant during the time course of the reaction.

Figure 5 represents a typical elution profile of the incubation mixture over a period of 15 minutes, it also shows that the disappearance of the nicotinate peak occurs concomitant with that of ATP. This coordinate relationship is illustrated quantitatively in Figure 6. As shown in Figure 6, the initial velocity for the two substrate disappearances and the two product appearances are equivalent until the PRPP concentration in the incubation mixture is exhausted. Thus, ADP and

Figure 3. Elutions of a stock solution of ATP, ADP, nicotinate, and N_aMN through a u-Bondapak C_{18} column using 25 mM $(NH_4)_3PO_4$ over a range of pH values. Stock solutions of each reactant were used to assign the peaks (the assignments of which are shown in Figure 4). Elution conditions: 5 ul sample injection volumes, 0.7-ml/min flow rate 25°C.

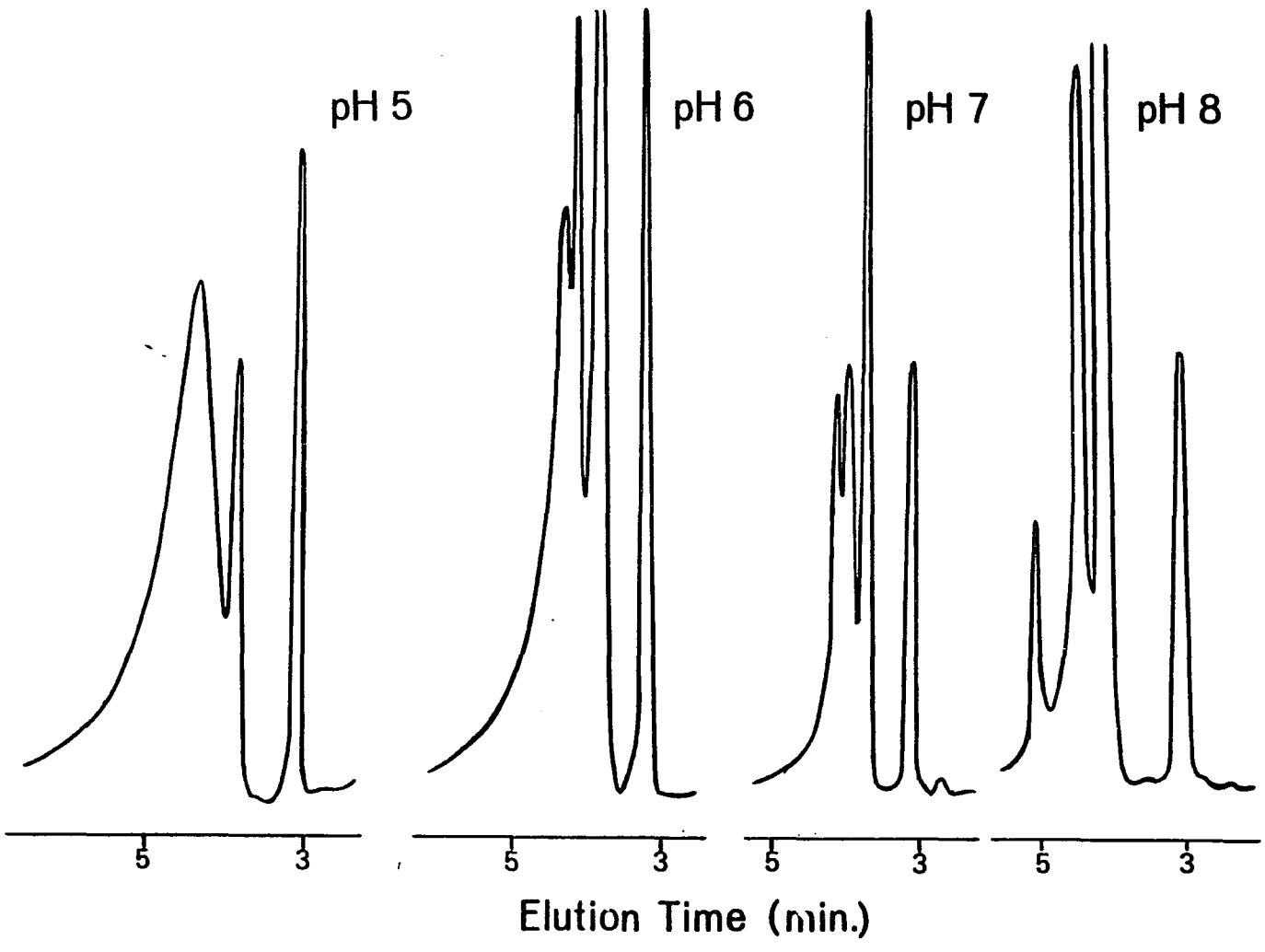
pH 5
pH 6
pH 7
pH 8
5
3
5
3
5
3
5
3
Elution Time (min.)

Figure 4. Measurements of the area under the absorption peaks following an elution of standard samples of known concentration through a u-Bondapak C_{18} column (top) and measurements of the peak heights following these same elutions (bottom). Elution conditions: 5 ul sample injection volumes, 0.7-ml/min flow rate, 25 mM $(NH_4)_3PO_4$ (pH 8) elution buffer, 25°C.

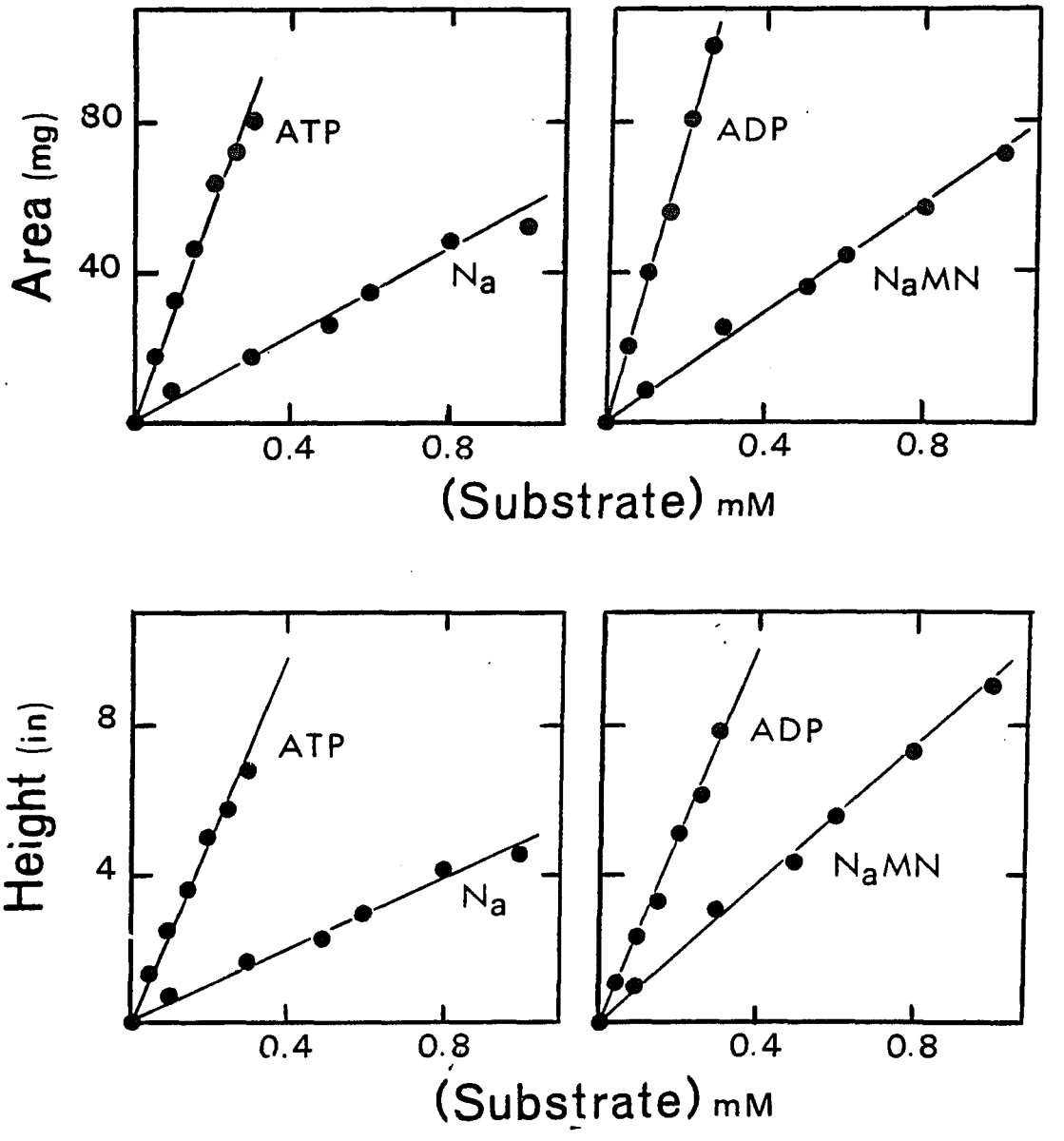
Area (mg)
80
40
ATP
Na
ADP
NaMN
0.4
0.8
0.4
0.8
(Substrate) mM
Height (in)
8
4
ATP
Na
ADP
NaMN
0.4
0.8
0.4
0.8
(Substrate) mM

Figure 5. Elutions of the nicotinate phosphoribosyltransferase (N_aPRTase) assay solution through a u-Bondapak C_{18} column after various incubation times. The incubation mixture contained 5 mM $MgCl_2$ 100 uM nicotinate, 75 uM ATP, 30 uM PRPP, and 25 ul of 4-mg/ml N_aPRTase in 50 mM Tris/phosphate (pH 8). The reaction was initiated and terminated after each incubation time as described under "Methods". Elution conditions: 5 ul sample injection volumes, 0.7-ml/min flow rate, 25 mM $(NH_4)_3PO_4$ (pH 8) elution buffer, 25°C.

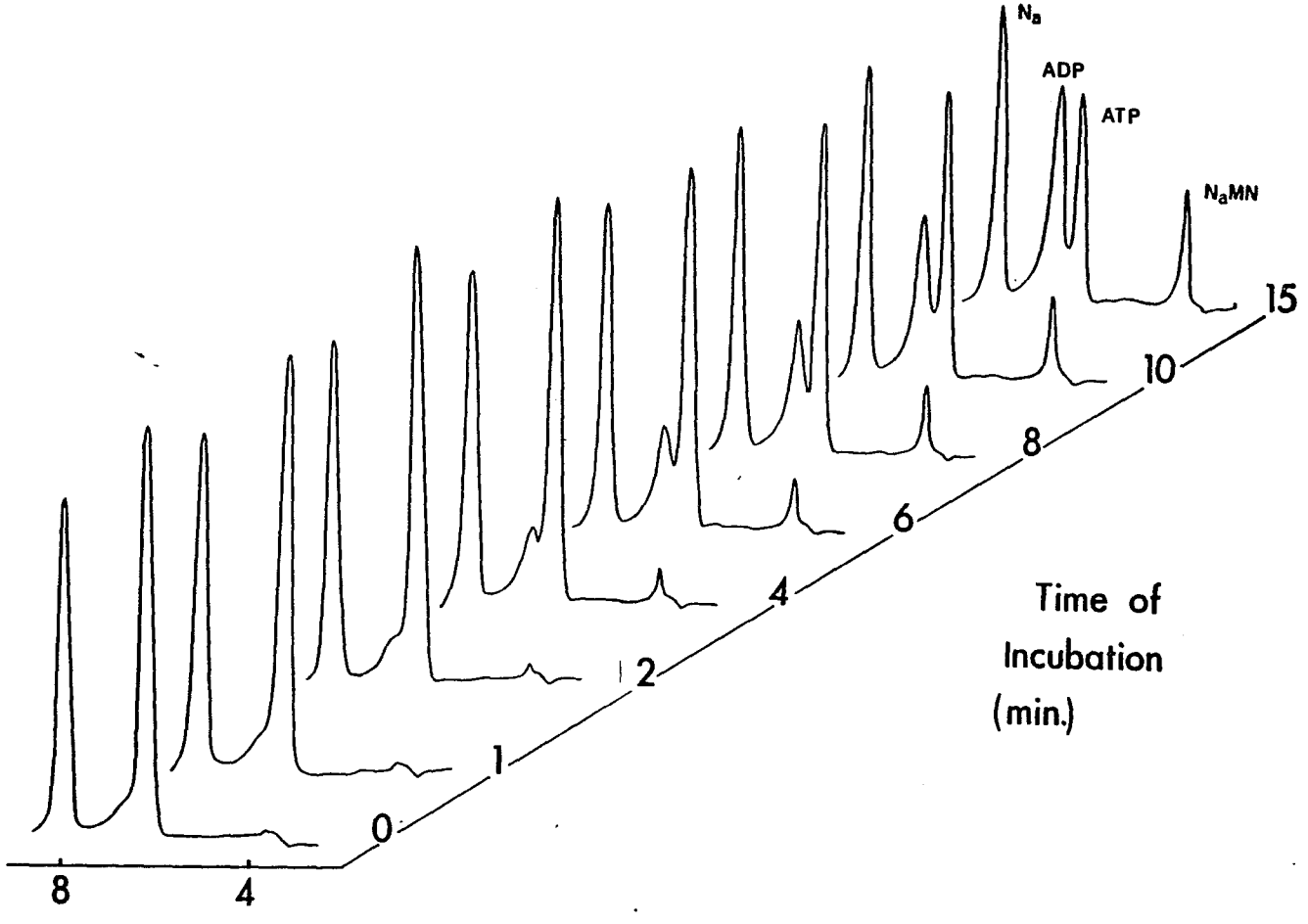
N_a
ADP
ATP
N_aMN
15
10
8
6
4
2
1
0
Time of
Incubation
(min.)
8
4

Figure 6. Time-dependent changes in the concentrations of N_aMN (solid circles), nicotinate (open circles), ATP (solid triangles), and ADP (open triangles) over a 15-min incubation with N_aPRTase as determined by elutions of aliquots of the incubation solution through a u-Bondapak C_{18} column. The incubation solution contained 5 mM $MgCl_2$, 60 uM ATP, 100 uM nicotinate, and one of the following concentrations of PRPP: 100 uM (A), 60 uM (B), 40 uM (C), 20 uM (D), 16 uM (E), 12 uM (F), 6 uM (G), or 4 uM (H). Elution conditions: 5 ul sample injection volumes, 0.7-ml/min flow rate, 25 mM $(NH_4)_3PO_4$(pH 8) elution buffer, 25°C.

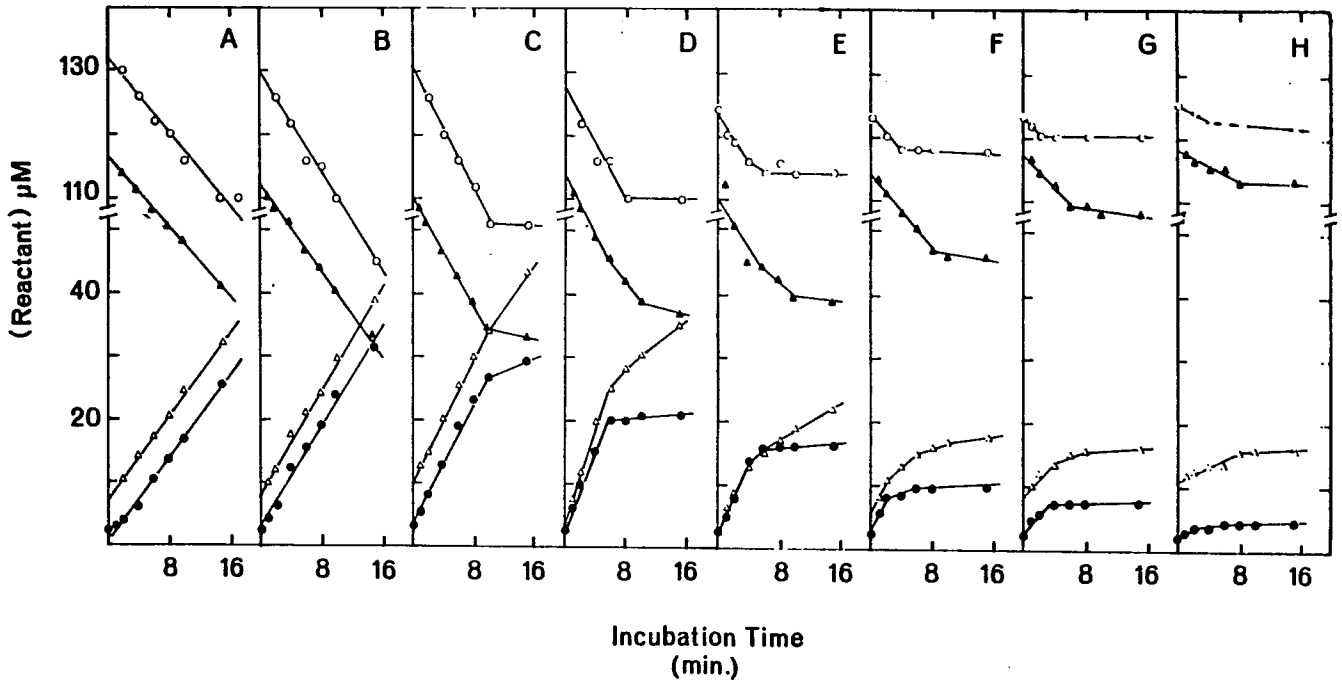
A
B
C
D
E
F
G
H
130
110
40
20
8
16
(Reactant) μM
Incubation Time
(min.)

N_aMN are formed to the same extent at an equivalent velocity. ATP hydrolysis continues in the absence of PRPP but at a greatly reduced rate. The significance of this observation will be discussed later.

Enzyme Purification

N_aPRTase from 48 pounds of baker's yeast was purified according to the procedure described in the "Methods" section. Table 1 illustrates the total protein, total activity, specific activity and the yield for every step in the purification procedure.

The purified N_aPRTase was homogeneous by the criteria of polyacrylamide gel electrophoresis (Figure 7), SDS gel electrophoresis (Figure 8) and isoelectric focusing gel electrophoresis (Figure 9). As shown in Figure 8, SDS gel electrophoresis performed in the presence and absence of mercaptoethanol shows one band of protein which has a molecular weight of approximately 45,000 as determined using separate runs with proteins of known molecular weights. Since Kosaka et al.[24] have shown that N_aPRTase from yeast has a molecular weight of 43,000 using a Sephadex G-100, this result demonstrates that N_aPRTase isolated from baker's yeast consists of a single polypeptide with molecular weight of 45,000±2000. As shown in Figure 9, isoelectric focusing gel electrophoresis experiments with N_aPRTase also provided a single protein band which focused at pH 6.9±0.3 (presumably the pI of this enzyme). Figure 10 illustrates a slab gel electrophoresis run for all different steps in the purification procedure. In this experiment samples from different steps were applied in duplicate. Two hydroxylapatite columns were utilized in this particular preparation. Later, I observed that one hydroxylapatite chromatographic step would suffice. In addition

Table 1. Purification of nicotinate phosphoribosyltransferase from baker's yeast

Step	Total Protein mg	Total Activity units*	Specific Activity units/mg	Yield %
1) Autolysis	984,000	5,040	0.005	--
2) Ammonium sulfate fractionation	446,000	3,200	0.007	--
3) $MnCl_2$ fractionation	312,000	6,820±	0.02	100.0
4) Ethanol fractionation	74,000	5,940	0.08	87.0
5) Phosphocellulose Chromatography	5,750	884	0.15	13.0
6) Hydroxylapatite Chromatography	3,100	510	0.17	7.5
7) Blue-Sepharose Chromatography	400	420	1.10	6.2
8) DEAE-Cellulose Chromatography	80	350	4.4	5.1

* 1.0 Unit = 1 u mol of N_aMN formed/min with the standard radioactive assay procedure described under "Methods".

± Considered as 100% yield. Allosteric inhibitors of $N_aPRTase$ might be removed at step 3.

Figure 7. Polyacrylamide disc gel electrophoresis of purified N_aPRTase from baker's yeast. 50 ug and 25 ug protein samples were placed onto gel A and B respectively. Polyacrylamide gel electrophoresis was then performed by the method of Davis[54] utilizing 7.5% polyacrylamide gel preparations at room temperature and at pH 8.9 and 4 mA/gel current. Protein was stained with Coomassie blue and destained in 10% acetic acid and 30% ethanol solution. Gel A was then scanned spectrophotometrically at 500 nm (C).

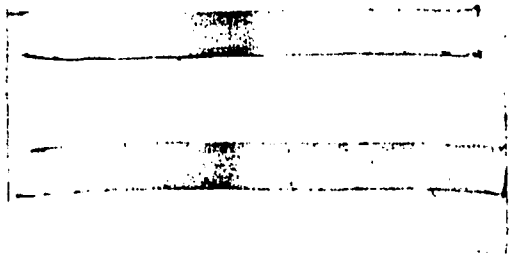
A
B

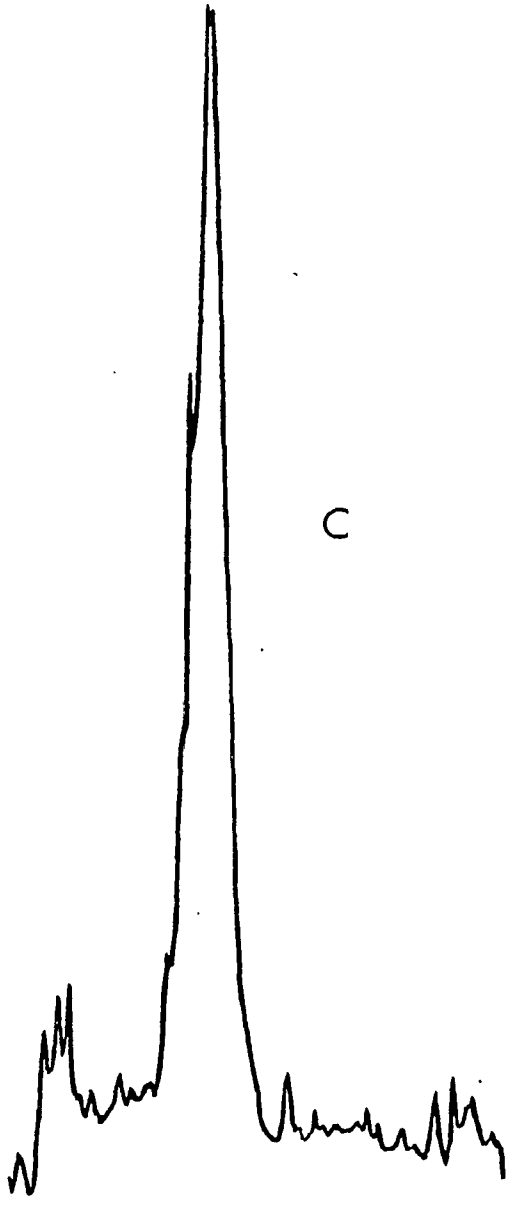
C

Figure 8. SDS-Polyacrylamide disc gel electrophoresis of purified N_aPRTase from baker's yeast. Protein (50 ug) in 1% solution of SDS was placed onto gel A (in the presence of mercaptoethanol) and on gel B (in the absence of mercaptoethanol). Experiments were performed by a modified procedure[55] of Shapiro et al.[56] Protein was stained with Coomassie blue and destained in 10% acetic acid and 30% ethanol solution. Gel A was then scanned spectrophotometrically at 500 nm (C).

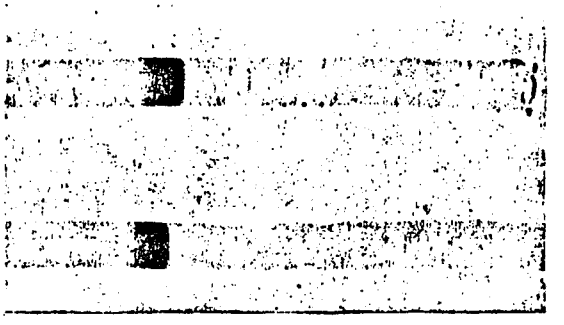

A

B

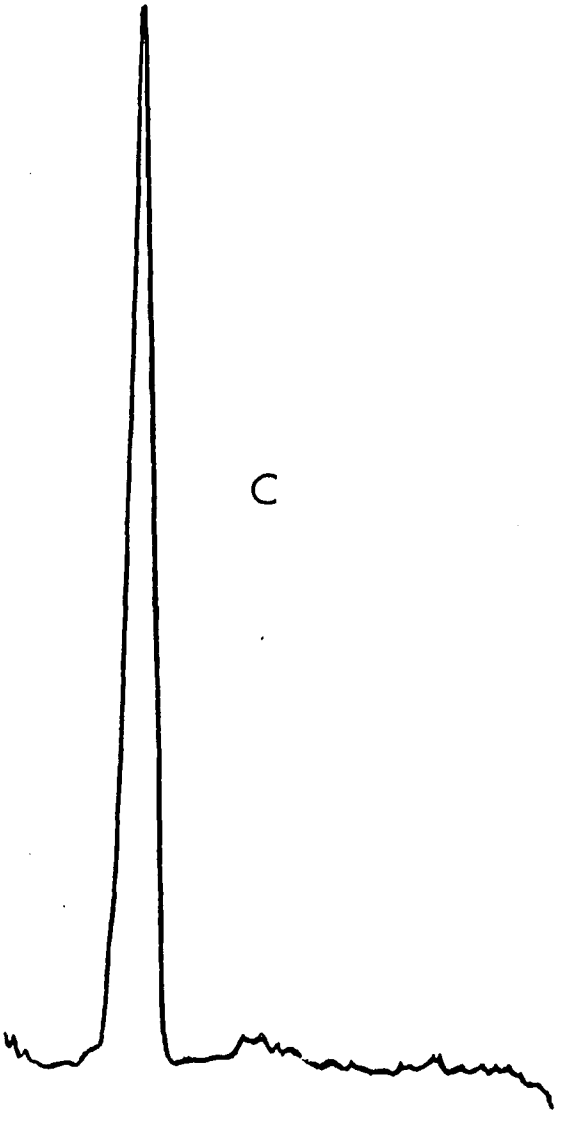

C

Figure 9. Polyacrylamide gel isoelectrofocusing of: A) 50 ug hemoglobin, B) 50 ug BSA and (C-E) purified N_aPRTase from baker yeast. 50 ug (C and E) and 30 ug (D) samples of the enzyme were employed. The samples were placed onto the gels and the experiment was carried out at 30 volt per gel by the method of Wrigley.[57] Gels were immersed in 10% trichloroacetic acid for 48 hours and stained with Coomassie blue in the presence of 0.1% copper (II) sulfate and then destained in 10% acetic acid and 25% ethanol solution. Gel E was scanned spectrophotometrically at 500 nm (F).

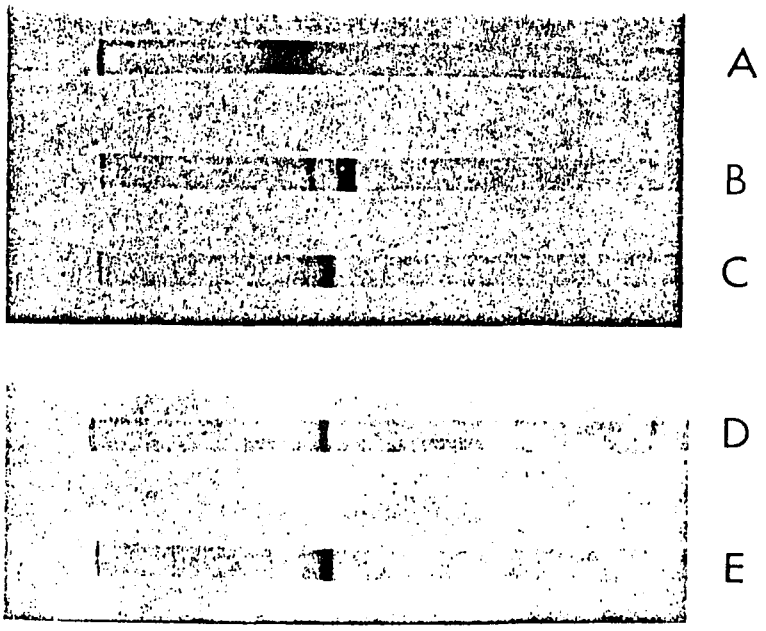
A
B
C
D
E
F

Figure 10. Slab gel polyacrylamide electrophoresis at different stages of N_aPRTase purification. Approximately 50 ug of protein were placed into the slots in duplicate: A) Autolysate, B) Redissolved ammonium sulfate precipitate, C) $MnCl_2$ fractionation supernatant, D) Redissolved ethanol precipitate, E) Pooled active phosphocellulose fractions, F) Pooled active hydroxylapatite chromatography fractions, G) Pooled active hydroxylapatite chromatography fractions before which the enzyme was incubated with the substrates PRPP and N_A, H) Pooled active Blue-Sepharose CL-6B chromatography fractions, I) and J) Pooled active DEAE-cellulose fractions from two analogous preparations. Polyacrylamide electrophorosis was performed utilizing 7.5% polyacrylamide gel preparation at 10° C at pH 8.9 and 40 mA current. Protein was stained with Coomassie blue and destained in 10% acetic acid and 30% ethanol solution.

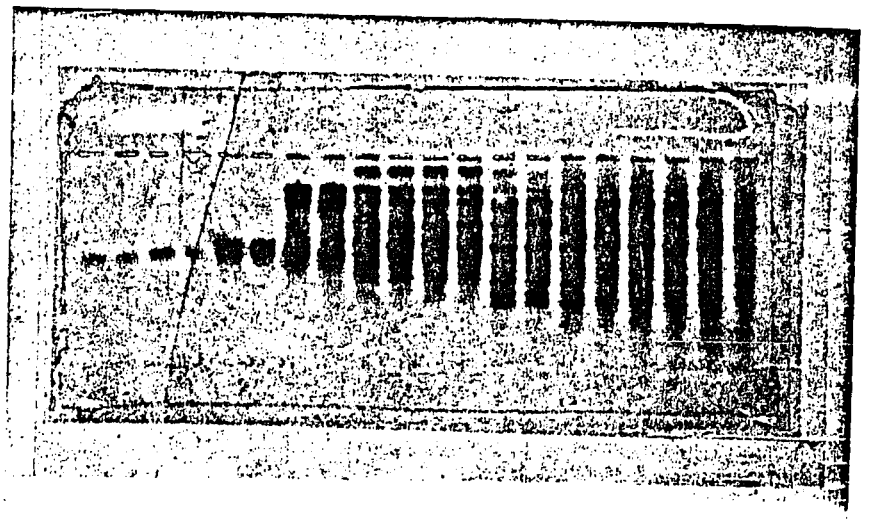

J I H G F E D C B A

(Figure 10), samples from two purified preparations were applied to the slab to show the consistency of the procedure.

Kinetic Analysis of N_aPRTase

1. Initial velocity double-reciprocal plots: Initial velocities (v) of the N_aPRTase catalyzed reaction were measured over a range of PRPP concentrations at four different ATP concentrations and at a fixed concentration of nicotinic acid. Substrate and product concentration changes observed using HPLC were averaged to arrive at a single value for v for each measurement. Double-reciprocal plots of (v) vs PRPP concentration at the four ATP concentrations are shown in Figure 11. Two interesting features of the reaction are illustrated in this plot: 1) There appears to be considerable inhibition of ATP function at relatively high concentrations of PRPP and at all concentrations of ATP. The inhibition is most pronounced at low ATP concentrations, suggesting that PRPP competes with ATP for the ATP binding site on the enzyme; 2) At relatively low PRPP concentrations a pattern of parallel lines is observed. This preliminary study was performed with partially purified N_aPRTase to demonstrate the reliability of the HPLC assay procedure.

This study was repeated with homogeneous enzyme and HPLC elution buffer at pH 6.0, after which the initial velocity (v) was calculated based on the average of the concentration changes of N_aMN and ATP. Again a slow hydrolysis of ATP was observed after PRPP had been exhausted and N_aMN formation had ceased, and again substrate inhibition was observed at high concentrations of PRPP. Figure 12 shows double-reciprocal plots of the initial velocities vs varied concentrations of

Figure 11. Double-reciprocal plots of PRPP concentration on the assay solution vs. the initial velocity (v) of the N_aPRTase catalyzed reaction in the presence of various concentrations of ATP. Each data point represents, as determined by the HPLC assay procedure, an average of the calculated rates of N_aMN, ATP, nicotinate, and ADP concentration changes. ATP concentrations used in these experiments were 240 uM (solid circles), 120 uM (solid triangles), 60 uM (open circles) and 30 uM (open triangles). The incubation solution contained 5 mM $MgCl_2$ and 100 uM nicotinate in 50 mM Tris/phosphate (pH 8) buffer. The reaction was initiated and terminated over a series of incubation times as described under "Methods". Elution conditions: 5 ul sample injection volumes, 0.7-ml/min flow rate, 25 mM $(NH_4)_3PO_4$ (pH 8) elution buffer, 25°C.

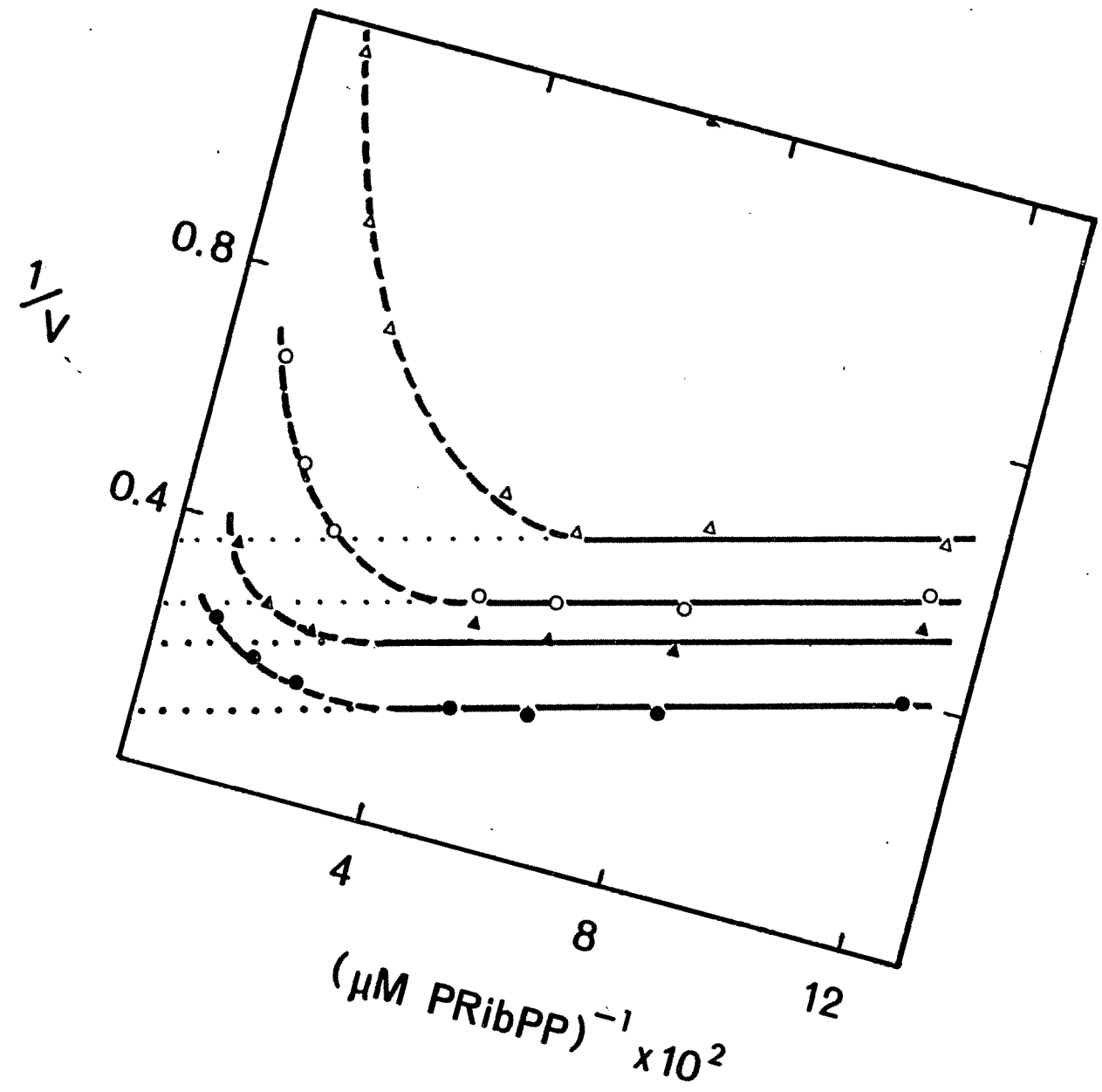
0.8
0.4
1/V
4
8
12
(μM PRibPP)⁻¹ x 10²

ATP at different values of PRPP (A) and vs varied concentrations of PRPP at different values of ATP (B). A constant concentration of nicotinic acid was used throughout these experiments. In Figure 12 we illustrate the measurements carried out at low (40 uM) concentrations of PRPP only where the above-described substrate inhibition effects were not observed. These lines are deemed to be parallel (in spite of the fact that a point of intersection can be constructed far to the left of each graph) because the lowest concentrations of ATP and PRPP used in the experiments are equal to or far less than the calculated K_m values for these substrates (vide infra). Although not shown in Figure 12, the plots of Y-intercepts of each graph vs the reciprocal of the concentrations of PRPP (A) or ATP (B) were linear.

Figure 13 shows double reciprocal plots of the initial velocities vs varied concentrations of ATP at different values of nicotinic acid (A) and vs varied concentrations of nicotinic acid at different values of ATP (B), and constant value of PRPP. Parallel sets of lines were obtained and the plots of Y-intercepts of each graph in Figure 13 vs the reciprocal of the concentrations of nicotinic acid (A) or ATP (B) were also linear. Figure 14 illustrates double reciprocal plots of the initial velocities vs varied concentrations of nicotinic acid at different values of PRPP (A) and varied concentrations of PRPP at different values of nicotinic acid (B). The concentrations of nicotinate used in these experiments were equal to or greater than this substrate's K_m value (in order to facilitate measurements of ATP concentration changes) and thus the point of intersection of the lines of graph 14A should be located far to the left of the graph. Nevertheless,

the lines do intersect, as exemplified by the line pattern of Figure 14B. In addition, the replots of $1/V_{max(app)}$ vs the reciprocal of the concentrations of PRPP (A) or nicotinic acid (B) (not shown) were observed to be linear.

According to the theoretical calculations presented by Segel,[68] the pattern observed (Figures 12, 13 and 14) are closest to the uni uni bi bi ter ter kinetic mechanism. However, one cannot exclude the hexa uni ping-pong ter ter kinetic mechanism. Moreover, the various kinetic constants could not be calculated from these initial velocity double reciprocal plots because there are three different variable unknowns in the velocity equation. In order to overcome this problem, two substrates must be maintained at constant ratio as has been suggested by Segel.[68] Thus such experiments were initiated.

Figures 15A and 15B show the double reciprocal plots of initial velocities vs varied concentrations of PRPP and nicotinic acid (maintained at constant ratio) at different concentrations of ATP. As shown in Figure 15, parallel sets of lines were obtained with a linear replot of $1/V_{max(app)}$ vs the reciprocal of the concentrations of ATP (Figure 15C). Figures 16A and 16B are double reciprocal plots of the initial velocities vs varied concentrations of ATP and nicotinic acid (maintained at constant ratio) at different concentrations of PRPP. The observed sets of lines appear to be parallel, however, the possibility that they can intersect at a point far to the left is present. The replot of the Y-intercepts vs the reciprocal of the concentrations of PRPP is linear (Figure 16C). A similar study of the double reciprocal plots of the initial velocities vs varied concentrations of

ATP and PRPP (maintained at constant ratio) at different concentrations of nicotinic acid is shown in Figures 17A and 17B. Intersecting line patterns are observed with a linear replot of the Y-intercepts vs the reciprocal of the nicotinic acid concentrations (Figure 17C).

These data were then replotted in a different manner, the double reciprocal plots of the initial velocities vs the concentrations of the varied substrate at different concentrations of the other two substrates maintained at constant ratio (Figures 18A, 19A and 20A). As shown in these three figures, plots of v^{-1} vs $[ATP]^{-1}$ and vs $[PRPP]^{-1}$ are composed of sets of parallel lines whereas a plot of v^{-1} vs $[N_A]^{-1}$ is composed of an intersecting-line pattern. The secondary plots of $V_{max(app)}{}^{-1}$ vs the reciprocal of the concentrations of each of the substrates that were maintained at constant ratio, were all linear (Figures 18B, 19B and 20B).

Table 2 defines the expected double-reciprocal line patterns and secondary plots, $V_{max(app)}{}^{-1}$ vs the reciprocal concentration of the appropriate substrate, based on theoretical calculations as presented by Segel.[68]

The experimentally-determined double reciprocal plots (Figures 12-20) and their secondary plots do not agree with the theoretical plots of any mechanism exclusively. Again, however, the observed double reciprocal plots may be considered to define (within the experimental error) a Uni Uni Bi Bi ping-pong Ter Ter mechanism.

To further investigate the possibility that this kinetic mechanism is the mechanism by which N_aPRTase proceeds, specific product inhibition studies were initiated.

Figure 12. Double-reciprocal plots of the initial velocity (v) vs. varied concentrations of ATP (A) and PRPP (B) in the assay of the N_aPRTase catalyzed reaction in the presence of different concentrations of PRPP (A) and ATP (B). Each data point represent (as determined by HPLC assay procedure) an average of the calculated rates of N_aMN and ATP concentrations changes. PRPP concentrations used in these experiments were 40 uM (Aa), 20 uM (Ab), 16 uM (Ac), 12 uM (Ad), 8 uM (Ac) and 4 uM (Af). ATP concentrations used were 240 uM (Ba), 120 uM (Bb), 60 um (Bc) and 30 uM (Bd). The incubation solutions contained 5 mM $MgCl_2$ and 100 uM nicotinic acid in 50 mM Tris-phosphate buffer at pH 8.0. The reaction was initiated and terminated over a series of incubation times as described under "Methods". Elution conditions: 5 ul sample injection volumes, 0.7 ml/min flow rate, 25 mM $(NH_4)_3PO_4$ pH 6.0 elution buffer, 25°C.

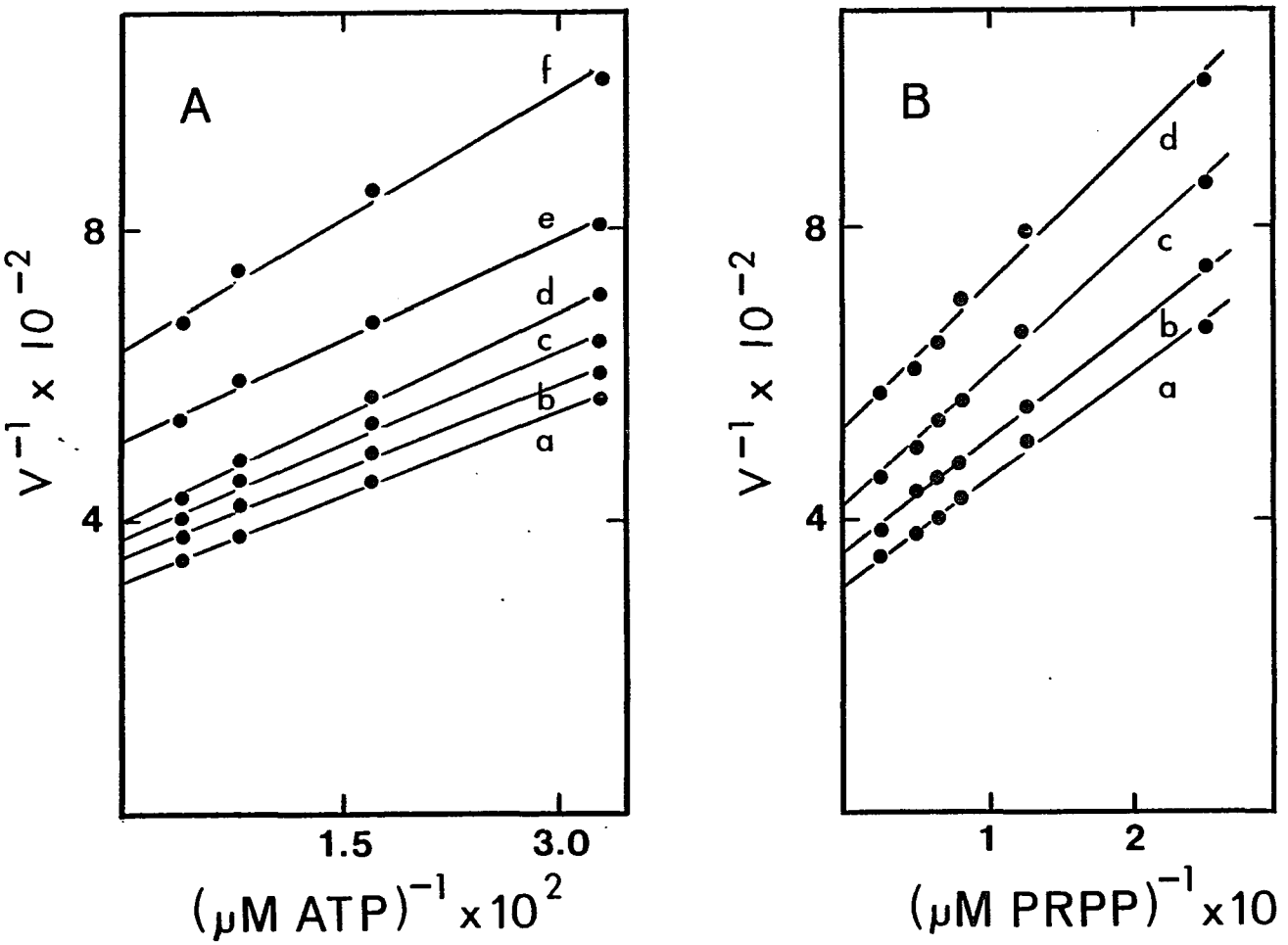
A
B
f
e
d
c
b
a
8
4
1.5
3.0
1
2
$V^{-1} \times 10^{-2}$
$(\mu M\ ATP)^{-1} \times 10^{2}$
$(\mu M\ PRPP)^{-1} \times 10$

Figure 13. Double-reciprocal plots of the initial velocity (v) vs. varied concentrations of ATP (A) and N_A (B) in the assay of the N_aPRTAse catalyzed reaction in the presence of different concentrations of N_A (A) and ATP (B). Each data point represents (as determined by HPLC assay procedure) an average of the calculated rates of N_aMN and ATP concentrations changes. N_A concentrations used in these experiments were 20, 40, 100 and 200 uM (A). ATP concentrations used were 30, 60 and 120 uM (B). The incubation solutions contained 5 mM $MgCl_2$ and 20 uM PRPP in 50 mM Tris-phosphate buffer at pH 8.0. The reaction was initiated and terminated over a series of incubation times as described under "Methods". Elution conditions: 5 ul samples injection volumes, 0.7 ml/min flow rate, 25 mM $(NH_4)_3PO_4$ pH 6.0 elution buffer, 25°C.

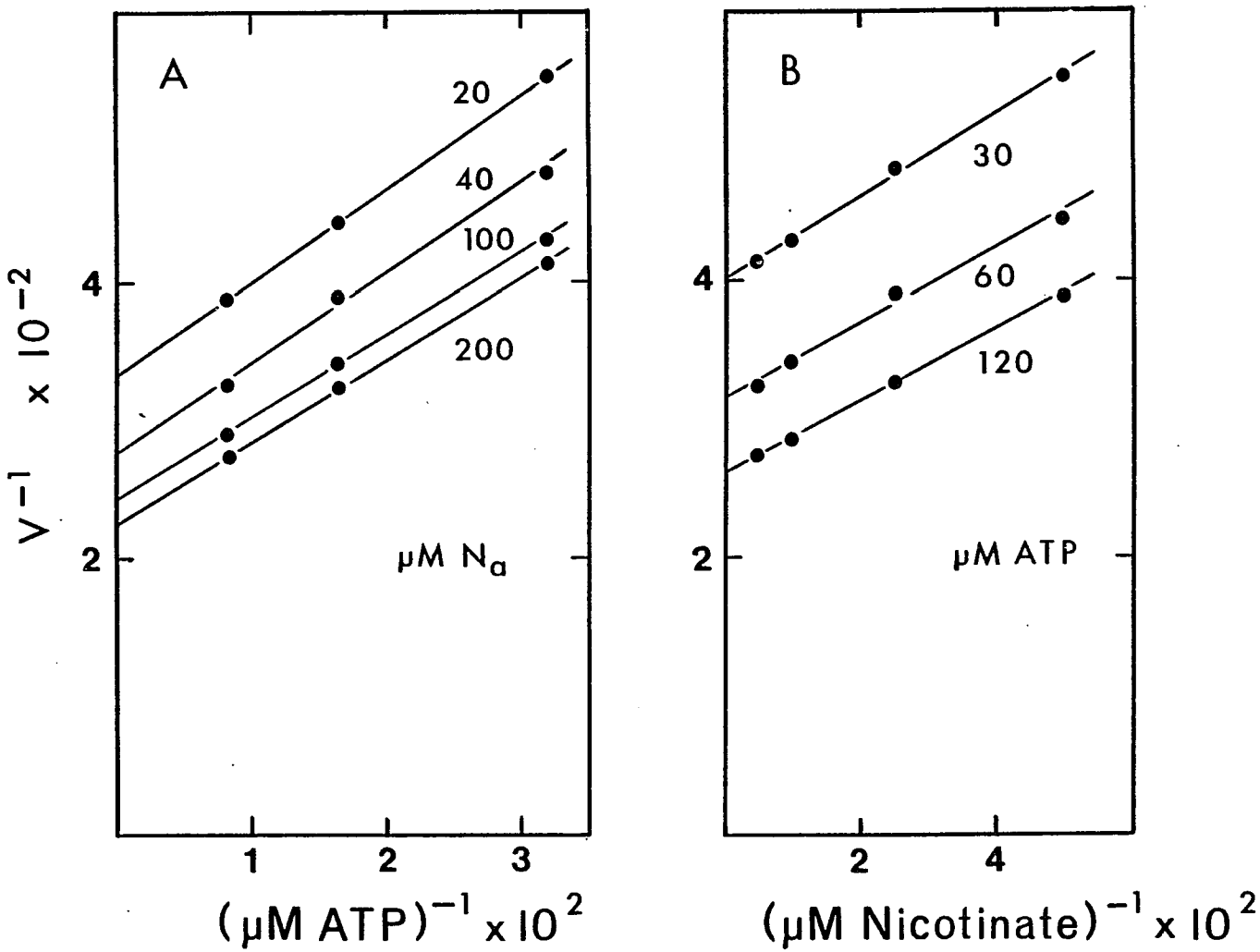
A
20
40
100
200
μM N_a
4
2
V^{-1} x 10^{-2}
1
2
3
(μM ATP)$^{-1}$ x 10^2
B
30
60
120
μM ATP
4
2
2
4
(μM Nicotinate)$^{-1}$ x 10^2

Figure 14. Double-reciprocal plots of the initial velocity (v) vs. varied concentrations of N_A (A) and PRPP (B) in the assay of the N_aPRTase catalyzed reaction in the presence of different concentrations of PRPP (A) and N_A (B). Each data point represents (as determined by HPLC assay procedure) an average of the calculated rates of N_aMN and ATP concentrations changes. PRPP concentrations used in these experiments were 80 uM (Aa), 40 uM (Ab), 20 uM (Ac), 16 uM (Ad), 12 uM (Ae), 8 uM (Af) and 4 uM (Ag). N_A concentrations used were 200 uM (Ba), 50 uM (Bb) and 20 uM (Bc). The incubation solutions contained 5 mM $MgCl_2$ and 240 uM ATP in 50 mM Tris-phosphate buffer at pH 8.0. The reaction was initiated and terminated over a series of incubation times as described under "Methods". Elution conditions: 5 ul samples injection volumes, 0.7 ml/min flow rate, 25 mM $(NH_4)_3PO_4$ pH 6.0 elution buffer, 25°C.

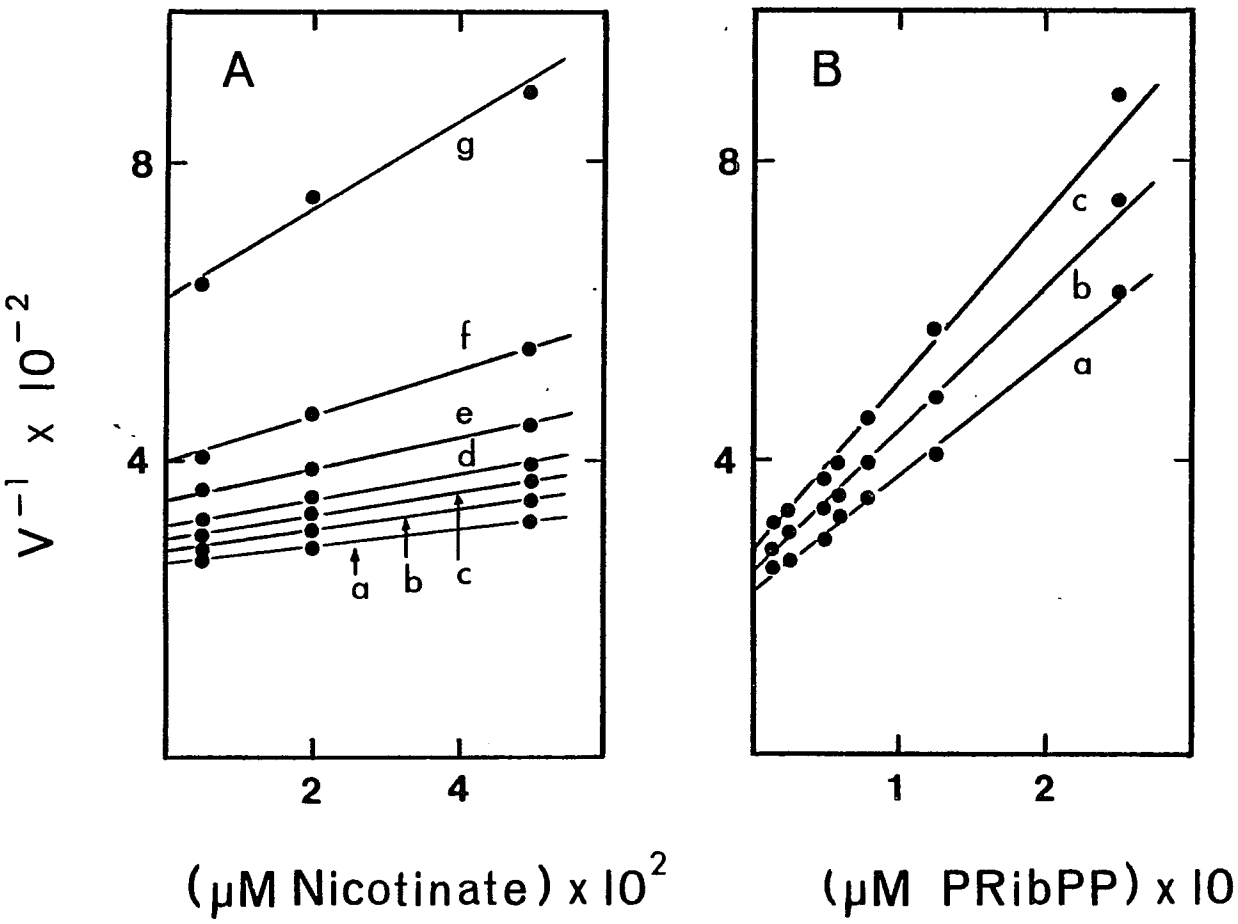
A
B
8
4
2
4
1
2
g
f
e
d
c
b
a
$V^{-1} \times 10^{-2}$
(μM Nicotinate) x 10^2
(μM PRibPP) x 10

Figure 15. Double-reciprocal plots of the initial velocity (v) vs varied concentrations of PRPP (A) and N_A (B) maintained at constant ratio (N_A = 5 x PRPP) in the assay of the N_aPRTase catalyzed reaction in the presence of various concentrations of ATP. Each data point represent (as determined by HPLC assay procedure) an avrage of the calculated rates of N_aMN and ATP concentration changes. ATP concentrations used in these experiments were 120 uM (a), 60 uM (b) and 30 uM (c). The incubation solutions contained 5 mM $MgCl_2$ and varied concentrations values of the N_A/PRPP ratio (20/4, 40/8, 80/16 and 160/32) in 50 mM Tris-phosphate buffer at pH 8.0. The reaction was initiated and terminated over a series of incubation times as described under "Methods". Elution conditions: 5 ul samples injection volumes, 0.7 ml/min flow rate, 25 uM $(NH_4)_3PO_4$ pH 6.0 elution buffer, 25°C. Figure 15C, is a replot of the Y-intercepts vs the reciprocals of the ATP concentration.

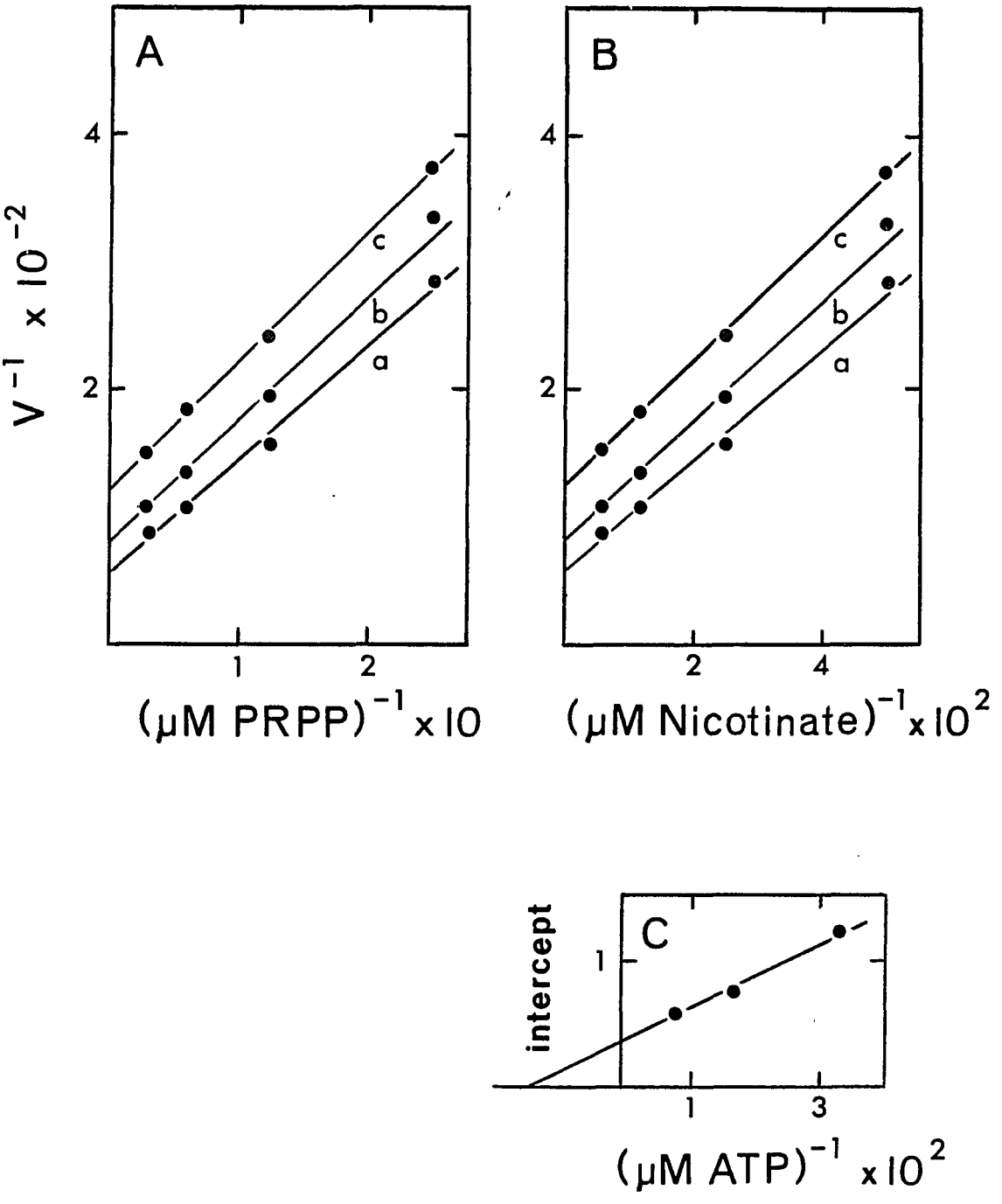
A
B
C
4
2
1
2
4
3
c
b
a
$V^{-1} \times 10^{-2}$
$(\mu M\ PRPP)^{-1} \times 10$
$(\mu M\ Nicotinate)^{-1} \times 10^{2}$
intercept
$(\mu M\ ATP)^{-1} \times 10^{2}$

Figure 16. Double-reciprocal plots of the initial velocity (v) vs varied concentrations of ATP (A) and N_A (B) maintained at constant ratio (N_A = 0.67 x ATP) in the assay of the N_aPRTase catalyzed reaction in the presence of various concentrations of PRPP. Each data point represents (as determined by HPLC assay procedure) an average of the calculated rates of N_aMN and ATP concentration changes. PRPP concentrations used in these experiments were 32 uM (a), 16 uM (b), 8 uM (c) and 4 uM (d). The incubation solutions contained 5 mM $MgCl_2$ and varied concentration values of the ATP/N_A ratio (30/20, 60/40, 120/80 and 240/160) in 50 mM Tris-phosphate buffer at pH 8.0. The reaction was initiated and terminated over a series of incubation times as described under "Methods". Elution conditions: 5 ul sample injection volumes, 0.7 ml/min flow rate, 25 mM $(NH_4)_3PO_4$ pH 6.0 elution buffer, 25°C. Figure 16C, is a replot of the Y-intercepts vs the reciprocals of the PRPP concentration.

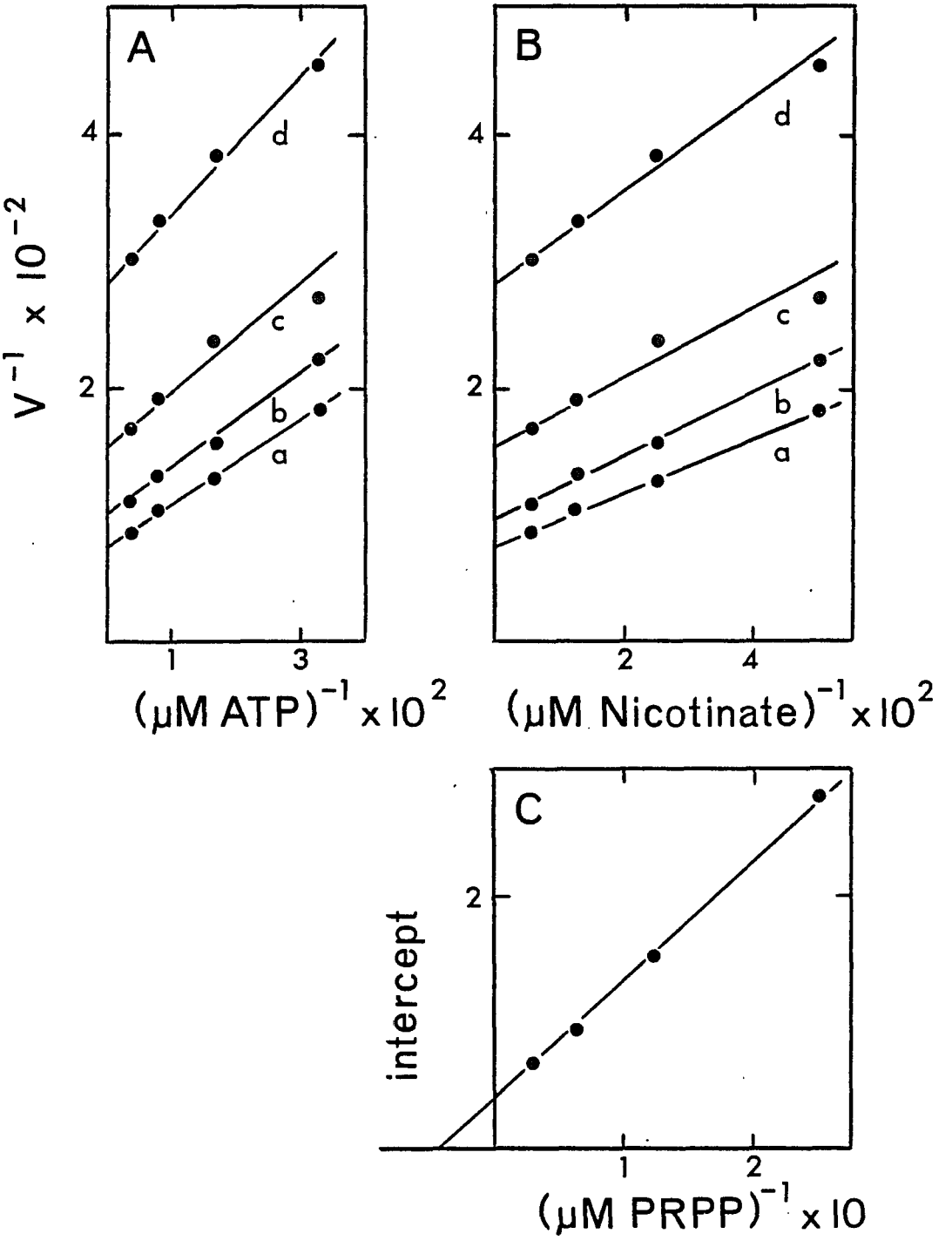
A
B
C
d
c
b
a
4
2
1
3
2
4
2
1
2
$V^{-1} \times 10^{-2}$
$(\mu M\ ATP)^{-1} \times 10^{2}$
$(\mu M\ Nicotinate)^{-1} \times 10^{2}$
intercept
$(\mu M\ PRPP)^{-1} \times 10$

Figure 17. Double-reciprocal plots of the initial velocity (v) vs varied concentrations of PRPP (A) and ATP (B) maintained at constant ratio (ATP = 7.5 x PRPP) in the assay of the N_aPRTase catalyzed reaction in the presence of various concentrations of N_A. Each data point represents (as determined by HPLC assay procedure) an average of the calculated rates of N_aMN and ATP concentration changes. Nicotinate concentrations used in these experiments were 80 uM (a), 40 uM (b) and 20 uM (c). The incubation solutions contained 5 mM $MgCl_2$ and varied concentration values of the ATP/PRPP ratio (30/4, 60/8, 120/16 and 240/32) in 50 mM Tris-phosphate buffer at pH 8.0. The reaction was initiated and terminated over a series of incubation times as described under "Methods". Elution conditions: 5 ul samples injection volumes, 0.7 ml/min flow rate, 25 mM $(NH_4)_3PO_4$ pH 6.0 elution buffer, 25°C. Figure 17C, is a replot of the Y-intercepts vs the reciprocals of the nicotinic acid concentration.

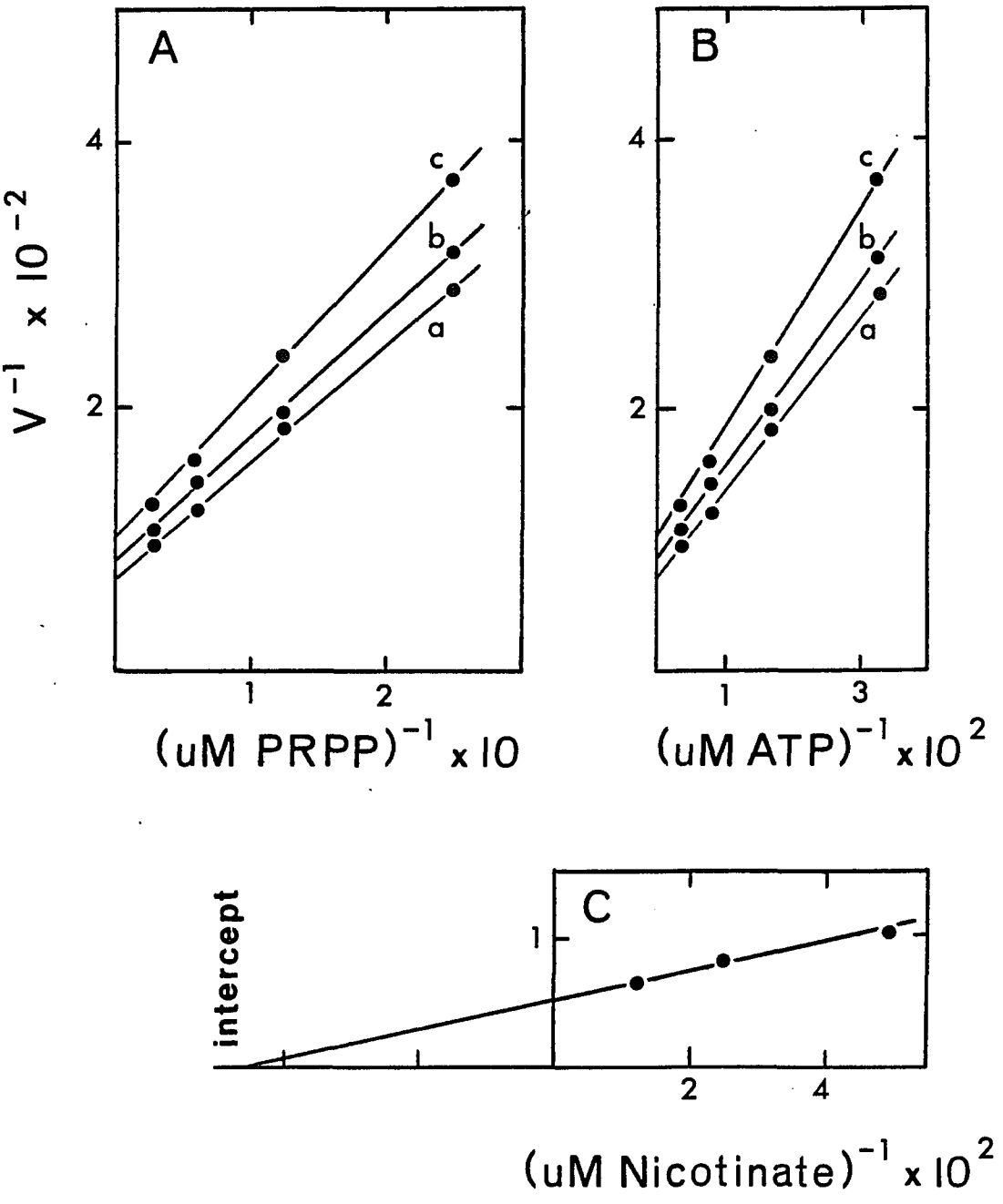
A
B
C
4
2
1
3
c
b
a
$V^{-1} \times 10^{-2}$
(uM PRPP)$^{-1}$ x 10
(uM ATP)$^{-1}$ x 10^{2}
intercept
(uM Nicotinate)$^{-1}$ x 10^{2}

Figure 18. A) Double-reciprocal plots of the initial velocity (v) vs varied concentrations of ATP in the assay of the N_aPRTase catalyzed reaction in the presence of various concentrations of PRPP and N_A maintained at constant ratio (N_A = 5 x PRPP). Each data point represents (as determined by HPLC assay procedure) an average of the calculated rates of N_aMN and ATP concentration changes. N_A/PRPP concentration ratios used in these experiments were 160/32 (a), 80/16 (b), 40/8 (c) and 20/4 (d). The incubation solutions contained 5 mM $MgCl_2$ and varied concentration values of ATP (30, 60 and 120 uM) in 50 mM Tris-phosphate buffer at pH 8.0. The reaction was initiated and terminated over a series of incubation times as described under "Methods". Elution conditions: 5 ul samples injection volumes, 0.7 ml/min flow rate, 25 uM $(NH_4)_3PO_4$ pH 6.0 elution buffer, 25°C. Figure 18B, is a replot of the Y-intercepts vs the reciprocals of the PRPP concentration.

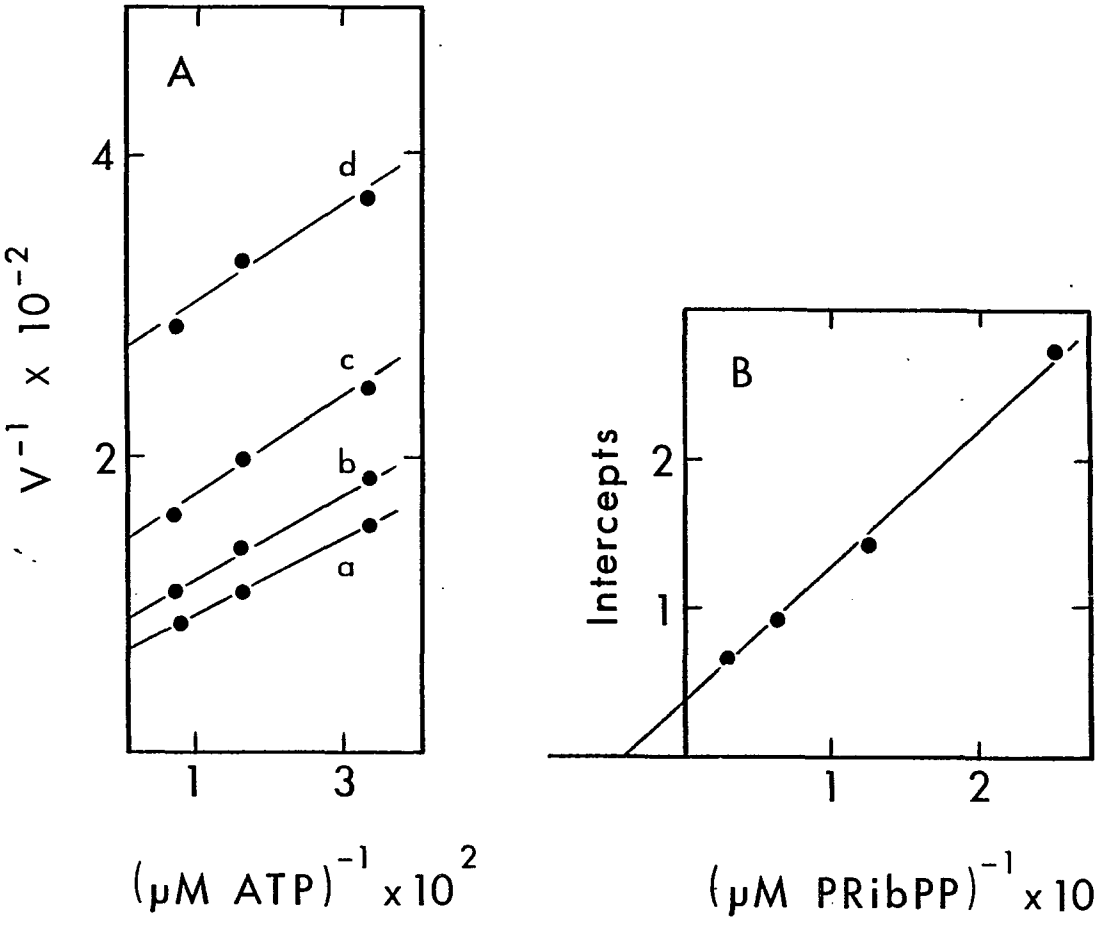
A
4
2
d
c
b
a
$V^{-1} \times 10^{-2}$
1
3
$(\mu M\ ATP)^{-1} \times 10^{2}$
B
Intercepts
2
1
1
2
$(\mu M\ PRibPP)^{-1} \times 10$

Figure 19. A) Double-reciprocal plots of the initial velocity (v) vs varied concentrations of PRPP in the assay of the N_aPRTase catalyzed reaction in the presence of various concentration of ATP and N_A maintained at constant ratio (N_A = 0.67 x ATP). Each data point represents (as determined by HPLC assay procedure) an average of the calculated rates of N_aMN and ATP concentration changes. N_A/ATP concentration ratios used in these experiments were 160/240 (a), 80/120 (b), 40/60 (c) and 20/30 (d). The incubation solutions contained 5 mM $MgCl_2$ and varied concentration values of PRPP (4, 8, 16, and 32 uM) in 50 mM Tris-phosphate buffer at pH 8.0. The reaction was initiated and terminated over a series of incubation times as described under "Methods". Elution conditions: 5 ul sample injection volumes, 0.7 ml/min flow rate, 25 mM $(NH_4)_3PO_4$ pH 6.0 elution buffer, 25°C. Figure 19B, is a replot of the Y-intercepts vs the reciprocals of the ATP concentration.

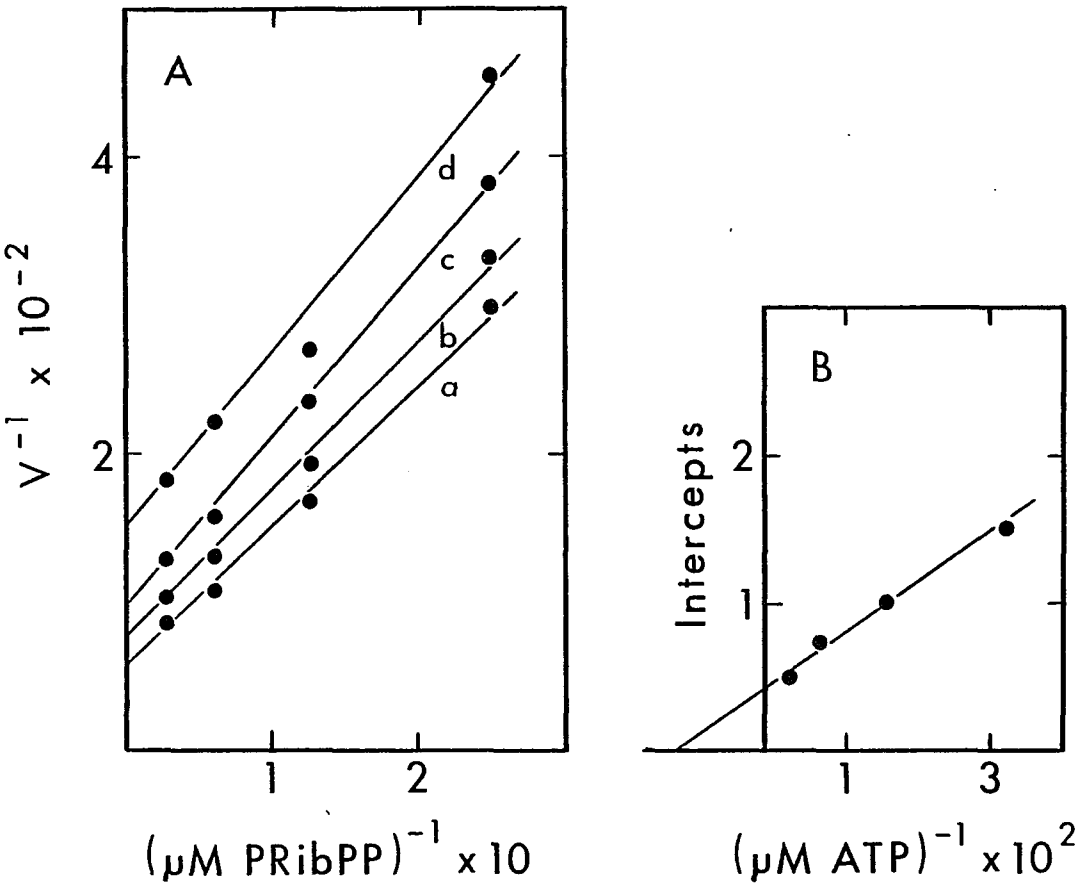
A
4
2
d
c
b
a
$V^{-1} \times 10^{-2}$
1
2
$(\mu M\ PRibPP)^{-1} \times 10$
B
Intercepts
2
1
1
3
$(\mu M\ ATP)^{-1} \times 10^{2}$

Figure 20. A) Double-reciprocal plots of the initial velocity (v) vs varied concentrations of N_A in the assay of the N_aPRTase catalyzed reaction in the presence of various concentrations of PRPP and ATP maintained at constant ratio (ATP = 7.5 x PRPP). Each data point represents (as determined by HPLC assay procedure) an average of the calculated rates of N_aMN and ATP concentration changes. ATP/PRPP concentration ratios used in these experiments were 240/32 (a), 120/16 (b), 60/8 (c) and 30/4 (d). The incubation solutions contained 5 mM $MgCl_2$ and varied concentration values of N_A (20, 40 and 80 uM) in 50 mM Tris-phosphate buffer at pH 8.0. The reaction was initiated and terminated over a series of incubation times as described under "Methods". Elution conditions: 5 ul sample injection volumes, 0.7 ml/min flow rate, 25 mM $(NH_4)_3PO_4$ pH 6.0 elution buffer, 25°C. Figure 20B, is a replot of the Y-intercepts, vs the reciprocals of the ATP concentration.

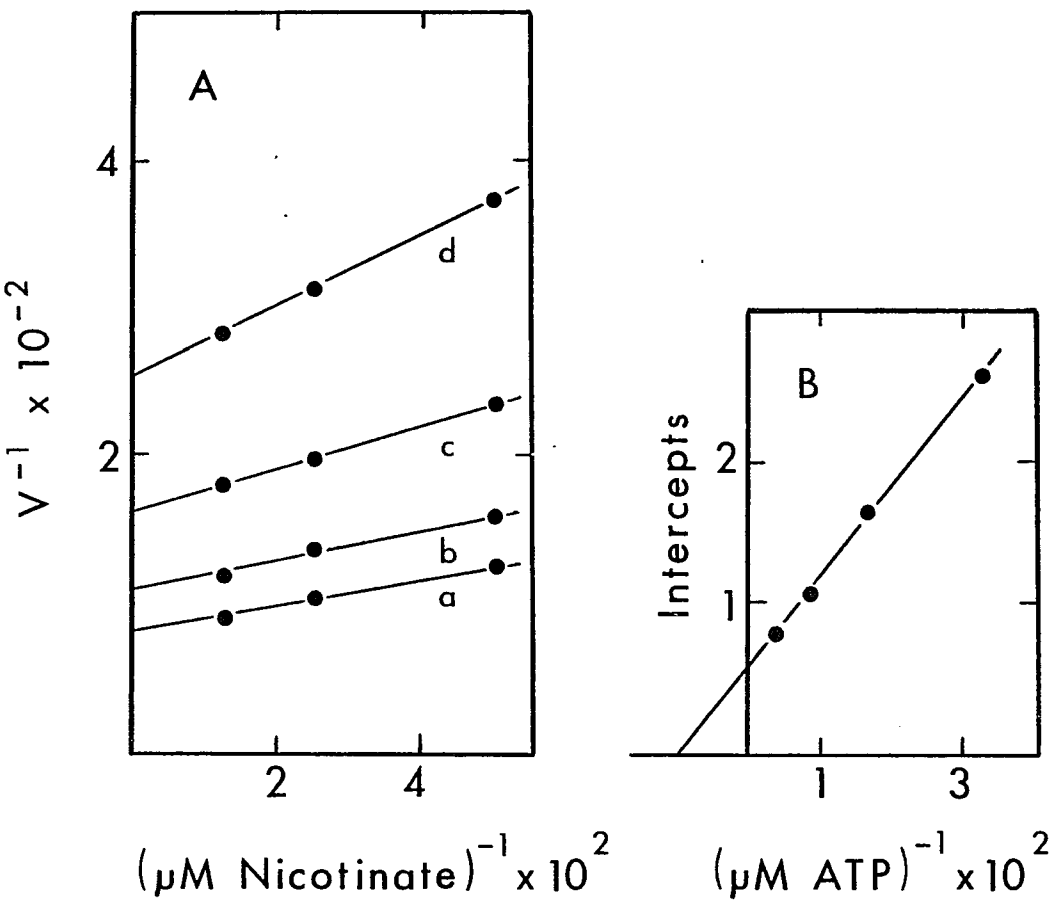
A
4
2
d
c
b
a
$V^{-1} \times 10^{-2}$
2
4
$(\mu M \text{ Nicotinate})^{-1} \times 10^{2}$
B
Intercepts
2
1
1
3
$(\mu M \text{ ATP})^{-1} \times 10^{2}$

Table 2. Double-reciprocal initial velocity patterns based on theoretical calculations as represented by Segel (68).

Procedure	Ordered Ter Ter	BiBi Uni Uni, Bi Uni Uni Bi & Bi Uni Uni Uni ping-pong	Hexa Uni ping-pong
Vary one substrate at different values the second substrate maintaining the third substrate constant.	Six sets of plots, all are linear and consist of intersecting line patterns.	Six sets of plots, all are linear and 4 consist of parallel line patterns and 2 consist of intersecting line patterns.	Six sets of plots, all are of linear and consist of parallel line patterns with linear secondary plots.*
Vary two substrates maintained at constant ratio at different values of the third substrate.	All sets of plots are parabolic with linear secondary plots of Y-intercepts.	Two sets of plots are linear and intersecting whereas the third set is parabolic. All produce linear secondary plots of Y-intercepts.	All sets of plots are linear and consist of parallel sets of lines with linear secondary plots of Y-intercepts.
Vary one substrate at different values of the other two substrates maintained at a constant ratio.	All sets of plots are linear and intersecting whereas two of the secondary plots are parabolic and one is linear.	All sets of plots are linear, two patterns consist of intersecting lines with linear secondary plots, a third pattern consists of parallel lines with a parabolic secondary plot.	All sets of plots are linear and consist of parallel sets of lines with linear secondary plots.

* Secondary plots are the plots of the Y-intercepts vs. the reciprocal concentration of the substrate held constant for the generation of each line of the pattern.

2. Product Inhibition Studies with Pyrophosphate

Double reciprocal plots of the initial velocity vs nicotinate concentrations at different concentrations of the product pyrophosphate (PP_i) at constant PRPP and ATP concentrations are shown in Figure 21. Mixed type patterns were observed at both conditions of saturated ATP (Figure 21A) and unsaturated ATP (Figure 21B) and where PRPP was kept constant at an unsaturated concentration (40 uM). Figure 22A shows a mixed type inhibition by the product pyrophosphate in a double reciprocal plot of (v) vs varied concentrations of PRPP at a constant and unsaturated value of ATP and a saturated value of nicotinate. Figure 22B and 22C illustrate the effects of increasing nicotinate concentration from an unsaturated level to a saturated level using double reciprocal plots of initial velocity vs varied concentrations of ATP in the presence of a constant concentration value of the product pyrophosphate and at constant and unsaturated level of PRPP. As shown in Figure 22B and 22C, mixed type patterns were observed at both saturated and unsaturated levels of nicotinate. Product inhibition at saturated levels of PRPP were not examined because such studies would not be of any importance in elucidating the kinetic mechanism (because of the substrate inhibition produced by high concentrations of PRPP). A summary of the product inhibition studies is represented in Table 3. In Table 4, are represented the expected line patterns for the product inhibiton studies for different types of kinetic mechanism based on theoretical calculations represented by Segel.[68]

Once again the obtained results are not in full agreement with any of the above patterns. However, if the order of substrate addition

is assumed to be ATP, PRPP and nicotinate in a Uni Uni Bi Bi ping-pong Ter Ter mechanism, then pyrophosphate may be assigned as the second product released (Q). These theoretical patterns (line 5 of Table 4) most closely resemble the observed results. One has to keep in mind that I am actually dealing with a ter quad system and not a ter ter system and that will have a profound effect on the product inhibition patterns. To explain the obtained product inhibition patterns, one has to follow three general rules; 1) if the product and the substrate bind to different forms of the enzyme, this product will affect the Y-intercept, 2) if the point of attachment of these two forms of enzyme are connected via a reversible sequence, this product will have a slope effect, 3) a product cannot affect either the slope or the Y-intercept for an enzyme form whose steady-state level is zero. In order to explain the obtained product inhibition patterns based on these rules, more information about the reversible steps in the reaction is required.

3. Isotope Exchange Studies

Because the initial velocity and product inhibition studies could not be used to eliminate the hexa-uni ping-ping mechanism as the kinetic mechanism by which N_aPRTase proceeds, isotope exchange studies between certain substrate/product pairs were initiated. Exchanges of label between nicotinate and N_aMN and between PRPP and PP_i would be expected during the course of such a mechanism.

A slow [^{14}C]-nicotinate/N_aMN exchange was observed in the presence of ATP and the absence of PRPP. No exchange has been observed in the

Figure 21. Product inhibition studies of N_aPRTase activity. Double reciprocal plots of the initial velocity (v) vs the nicotinate concentration in the presence of a different concentration values of the product pyrophosphate (PP_i) and saturated concentration of ATP (A) or unsaturated concentration of ATP (B). Each data point represents (as determined by HPLC assay procedure) an average of the calculated rates of N_aMN and ATP concentration changes. Pyrophosphate concentrations used in these experiments were 0 uM (a), 60 uM (b), 120 uM (c) and 240 uM (d). The incubation solutions contained 5 mM $MgCl_2$, 40 uM PRPP, varied concentrations of nicotinate (20, 40, 100 and 200 uM) and 1 mM ATP (A) and 60 uM ATP (B) in 50 mM Tris-phosphate buffer at pH 8.0. The reaction was initiated and terminated over a series of incubation times as described under "Methods". Elution conditions: 5 ul sample injection volumes, 07. ml/min flow rate, 25 mM $(NH_4)_3PO_4$ pH 6.0 elution buffer, 25°C.

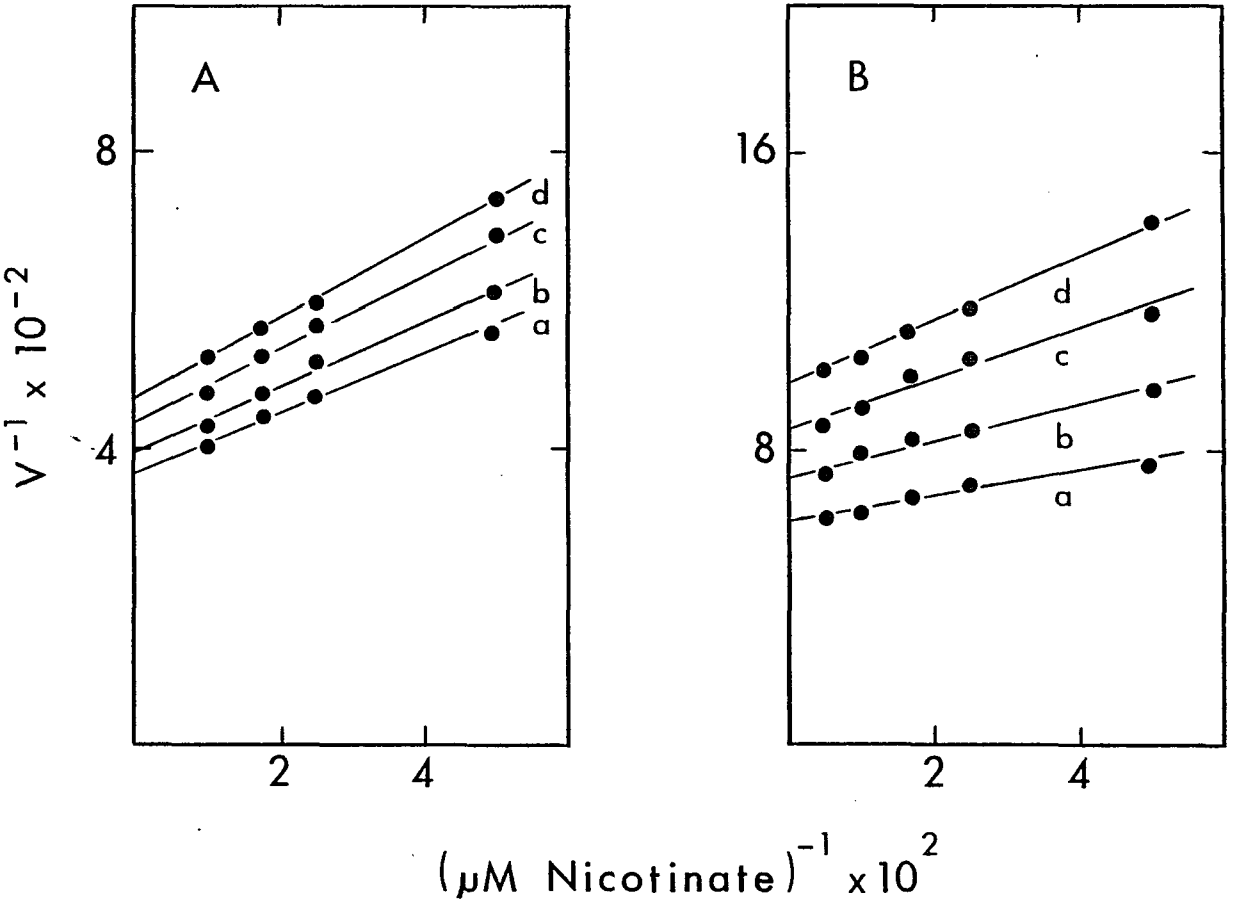
A
B
8
4
16
8
2
4
2
4
d
c
b
a
d
c
b
a
$V^{-1} \times 10^{-2}$
$(\mu M \text{ Nicotinate})^{-1} \times 10^{2}$

Figure 22. Product inhibition studies of N_aPRTase activity. Double reciprocal plots of the initial velocity (v) vs PRPP concentrations (A) and ATP concentrations (B and C) in the presence of different concentration values of the product pyrophosphate (PP_i). Each data point represents (as determined by HPLC assay procedure) an average of the calculated rates of N_aMN and ATP concentration changes. Pyrophosphate concentrations used in these experiments were 0 uM (Aa), 240 uM (Ab), 0 uM (Ba and Ca), 240 uM (Bb, Bc, Bd, Be and Cb) and 2000 uM (Cc and Cd). The incubation solutions contained A) 5 mM $MgCl_2$, 60 uM ATP and 600 uM nicotinate, B) 5 mM $MgCl_2$, 40 uM PRPP and varied concentrations of nicotinate, 600 uM (a and b), 400 uM (c), 200 uM (d) and 100 uM (e), C) 5 mM $MgCl_2$, 40 uM PRPP and varied concentrations of nicotinate, 600 uM (a, b, and c) and 100 uM (d), in 50 mM Tris-phosphate buffer at pH 8.0. The reaction was initiated and terminated over a series of incubation times as described under "Methods". Elution conditions: 5 ul sample injection volumes, 0.7 ml/min flow rate, 25 mM $(NH_4)_3PO_4$ pH 6.0 elution buffer, 25°C.

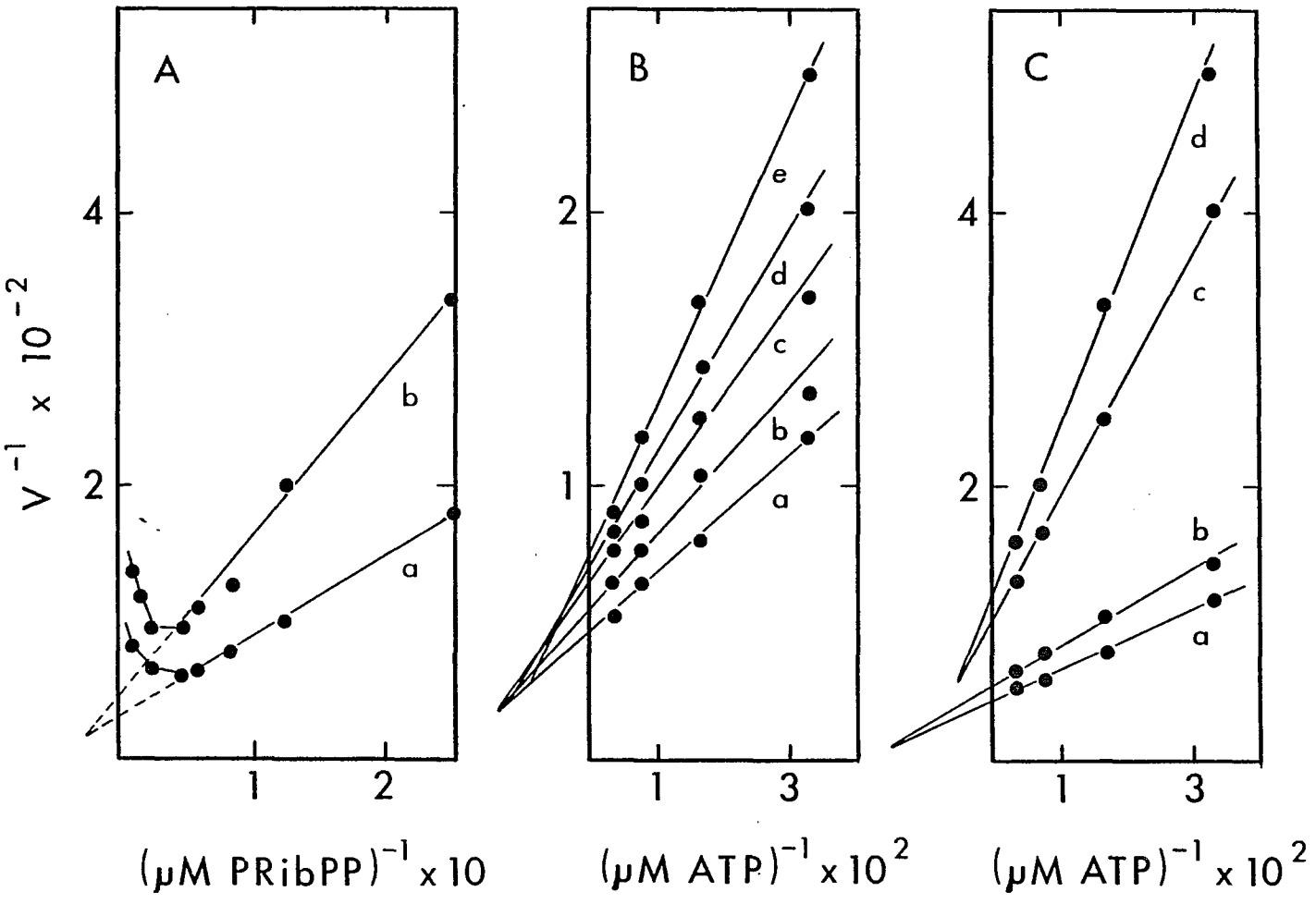
A
B
C
$V^{-1} \times 10^{-2}$
4
2
1
2
1
3
1
3
a
b
c
d
e
$(\mu M\ PRibPP)^{-1} \times 10$
$(\mu M\ ATP)^{-1} \times 10^{2}$
$(\mu M\ ATP)^{-1} \times 10^{2}$

Table 3. Product inhibition studies by pyrophosphate

Product	Varied Substrate						
	ATP			PRPP		Nicotinate	
	unsaturated	saturated	N_A	saturated nicotinate	unsaturated	saturated	ATP
Pyrophosphate	MT[a]	MT		MT(C)[b]	MT	MT	

[a] MT, mixed type, lines intersect at the left of the Y-axis.

[b] C, competitive type, lines intersect on the Y-axis.

Table 4. Product inhibition patterns based on theoretical calculations as represented by Segel.[68]

Mechanism	Product	Varied Substrate A			B			C		
		unsat.	sat. B	sat. C	unsat.	sat. A	sat. C	unsat.	sat. A	sat. B
Ordered Ter Ter	P	MT[a]	UC	UC	MT	MT	UC	MT	MT	MT
	Q	UC[b]	UC	UC	UC	UC	UC	UC	UC	UC
	R	C[c]	C	C	MT	--	MT	MT	--	UC
Uni Uni BiBi Ping-Pong Ter Ter	P	MT	--	MT	C	C	C	MT	MT	--
	Q	UC	UC	UC	MT	MT	UC	MT	MT	MT
	R	C	C	C	UC	--	UC	UC	--	UC
Hexa Uni Ping-Pong	R	MT	--	MT	C	C	C	UC	UC	--
	Q	UC	UC	--	MT	MT	--	C	C	C
	R	C	C	C	UC	--	UC	MT	--	MT

[a] MT, mixed type, lines intersect at the left of the Y-axis.

[b] UC, uncompetitive type, lines are parallel.

[c] C, competititve type, lines intersect on the Y-axis.

absence of ATP, and in the presence or absence of PRPP. Table 5 summarizes the total [^{14}C]-activity (of both nicotinate and N_aMN), the [^{14}C]-activity incorporated into N_aMN and the % activity after one hour incubation using different exchange conditions.

The % exchange seems to decrease with the increase of nicotinic acid concentrations, whereas it increased with the increase of N_aMN concentrations. Because of the slow rate of exchange seen (approximately 30 times slower than the rate of the reaction), further studies of this exchange were unnecessary at this stage. Furthermore, no exchange has been observed between [^{32}P]-pyrophosphate and PRPP under any condition (in the presence or absence of either ATP or nicotinate). Table 6 summarizes the [^{32}P]-count/minute of the top of PP_i peak and [^{32}P]-count/minute of the top of PRPP peak. Thus it would appear unlikely that a "ping-pong" step occurs during the course of the ribosyltransfer or pyrophosphorolysis reactions. However, these results may indicate that PRPP and nicotinate bind to the enzyme in order (where PRPP adds first) and that the inorganic phosphate group leaves the enzyme after N_aMN.

4. ATPase Activity of N_aPRTase

As was denoted previously, N_aPRTase catalyzes the hydrolysis of ATP to ADP and inorganic phosphate in the absence of the substrate PRPP but in the presence of either product pyrophosphate or N_aMN. This unique aspect of the N_aPRTase catalyzed reaction has been used to reveal portions of the kinetic mechanism of the enzyme. Figure 23 represents a typical elution profile of the incubaion mixture over

Table 5. Isotope exchange studies with [^{14}C]-N_A/N_aMN.

Additions	Total Activity	N_2MN Activity	% Activity
10 uM [^{14}C]-N_A, 1 mM N_aMN and 250 uM ATP	1) 17881.0	752.0	4.2
	2) 17825.0	728.0	4.1
40 uM [^{14}C]-N_A, 1 mM N_aMN and 250 uM ATP	1) 17633.0	583.0	3.3
	2) 17891.0	550.0	3.1
10 uM [^{14}C]-N_A and 1 mM N_aMN	1) 16682.0	198.0	1.2
	2) 16752.0	199.0	1.2
40 uM [^{14}C]-N_A and 1 mM N_aMN	1) 17391.0	207.0	1.2
	2) 17284.0	217.0	1.3
10 uM [^{14}C]-N_A, 1 mM N_aMN and 30 uM PRPP	1) 16940.0	319.0	1.9
	2) 17294.0	314.0	1.8
40 uM [^{14}C]-N_A, 1 mM N_aMN and 30 uM PRPP	1) 16934.0	284.0	1.7
	2) 16968.0	308.0	1.8
10 uM [^{14}C]-N_A, 1 mM N_aMN and 250 uM ATP in the absence of enzyme	1) 17904.0	312.0	1.7
	2) 17930.0	280.0	1.6

Table 6. Isotope exchange studies with [^{32}P]-PPi/PRPP.

Additions	[^{32}P]-PPi Activity	[^{32}P]-PRPP
0.5 mM [^{32}P]-PPi, 1 mM PRPP and 1 mM ATP	17,000	500
0.5 mM [^{32}P]-PPi, 3 mM PRPP and 3 mM ATP	17,000	600
0.5 mM [^{32}P]-PPi, 4 mM PRPP and 4 mM nicotinate	22,000	200
0.5 mM [^{32}P]-PPi and 4 mM PRPP	20,000	150
0.5 mM [^{32}P]-PPi, 3 mM PRPP and 3 mM ATP in the absence of enzyme	18,000	500

a period of 30 minutes for the ATPase activity of the N_aPRTase in the presence of pyrophosphate and the absence of both PRPP and nicotinate. It also shows the concomitant disappearance of ATP with the appearance of ADP. Figure 24 shows the breakdown of ATP with time under different conditions. N_aPRTase does not catalyze the hydrolysis of ATP in the absence or the presence of either PRPP or nicotinate and in the absence of the products pyrophosphate and N_aMN. Whereas in the presence of either pyrophosphate or N_aMN, N_aPRTase catalyzes the hydrolysis of ATP in the absence of PRPP and in the presence or absence of nicotinate. However, N_aPRTase will not demonstrate ATPase activity in the presence of pyrophosphate or N_aMN with the presence of PRPP. This may indicate that pyrophosphate and N_aMN bind to the PRPP binding site in order to trigger the ATPase activity. The fact that PRPP and not nicotinate inhibited this ATPase activity indicates that PRPP must bind before nicotinate. Moreover, one can conclude that pyrophosphate and N_aMN may leave the enzyme in random order and before the organic phosphate can leave the enzyme.

Figure 25 illustrates the pH profile of the ATPase activity triggered by pyrophosphate in the absence of PRPP and nicotinate. The N_aPRTase was shown to have maximum ATPase activity at pH range of 7-8.[24] Moreover, we have demonstrated in Figure 25 that just a change of pH in the absence of pyrophosphate failed to trigger the ATPase activity.

5. Cr^{III}-Pyrophosphate and Cr^{III}-ATP Inhibition Studies

One of the most difficult areas to define in many enzyme mechanisms, is the role of the metal ion activators. Some information can

Figure 23. Elutions of the N_aPRTase assay solution, in the absence of PRPP and nicotinate (which demonstrate the ATPase activity of the enzyme) through a u-Bondapak C_{18} HPLC column after various incubation times. The incubation mixture contained 5 mM $MgCl_2$, 60 uM ATP and 100 uM pyrophosphate in 50 mM Tris-phosphate buffer at pH 8.0. The reaction was initiated and terminated as described under "Methods". Elution conditions: 5 ul samples injection volumes, 0.7 ml/min flow rate, 25 mM $(NH_4)_3PO_4$ pH 6.0 elution buffer, 25°C.

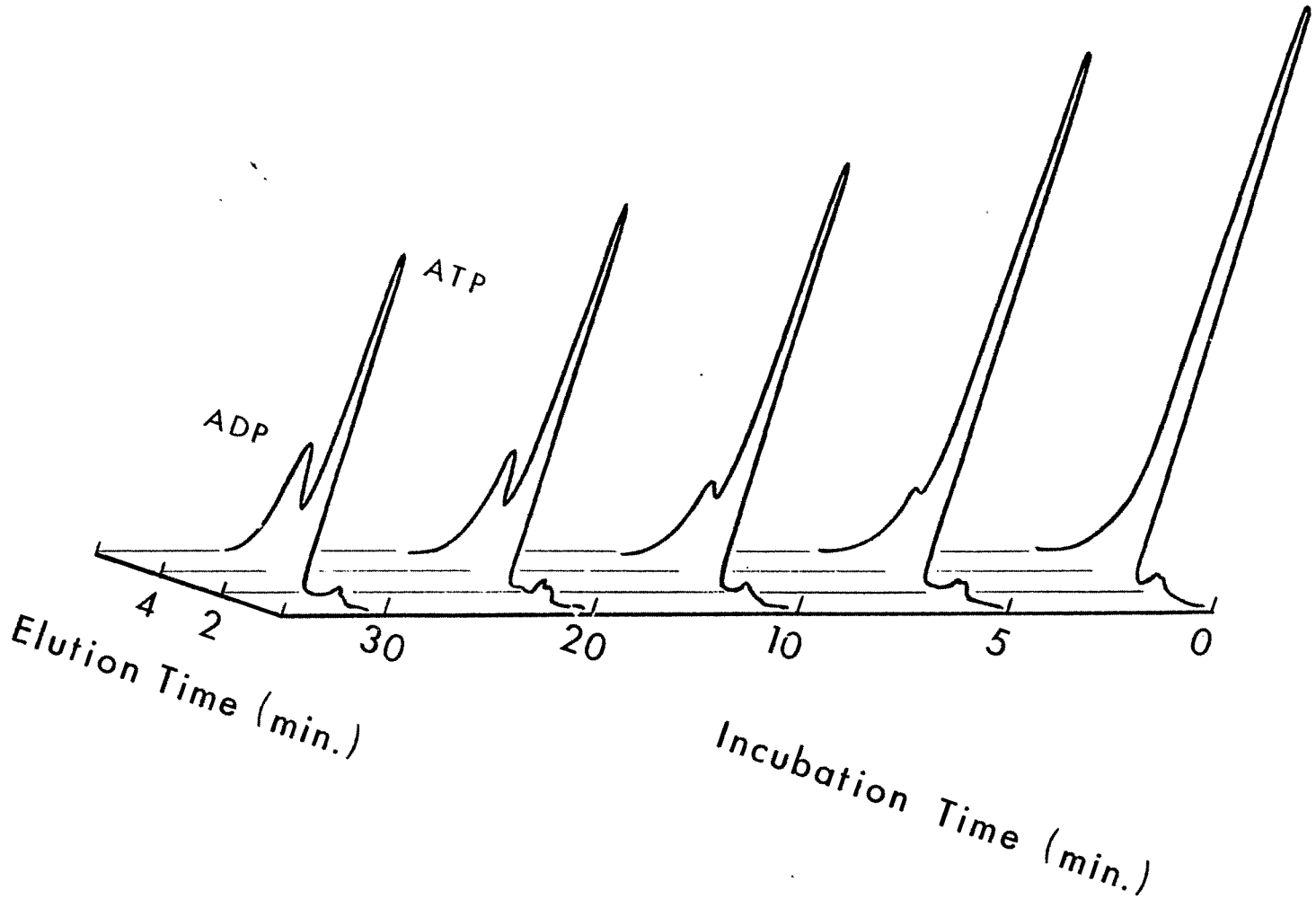
ATP
ADP
4
2
30
20
10
5
0
Elution Time (min.)
Incubation Time (min.)

Figure 24. Time-dependent changes in the concentration of ATP over a 30 minute incubation with N_aPRTase as determined by procedures described in Figure 23. The incubation solutions contained 5 mM $MgCl_2$, 60 uM ATP and the following: a) no further additions, b) 40 uM PRPP and 100 uM PP_i, c) 100 uM PP_i, d) 200 uM nicotinate, e) 200 uM nicotinate and 100 uM PP_i, f) 200 uM nicotinate and 100 uM N_aMN, g) 40 uM PRPP, h) 100 uM N_aMN and 40 uM PRPP and i) 100 uM N_aMN, in 50 mM Tris-phosphate buffer at pH 8.0. The reaction was initiated and terminated as described under "Methods". Elution conditions: 5 ul sample injection volumes, 0.7 ml/min flow rate, 25 mM $(NH_4)_3PO_4$ pH 6.0 elution buffer, 25°C.

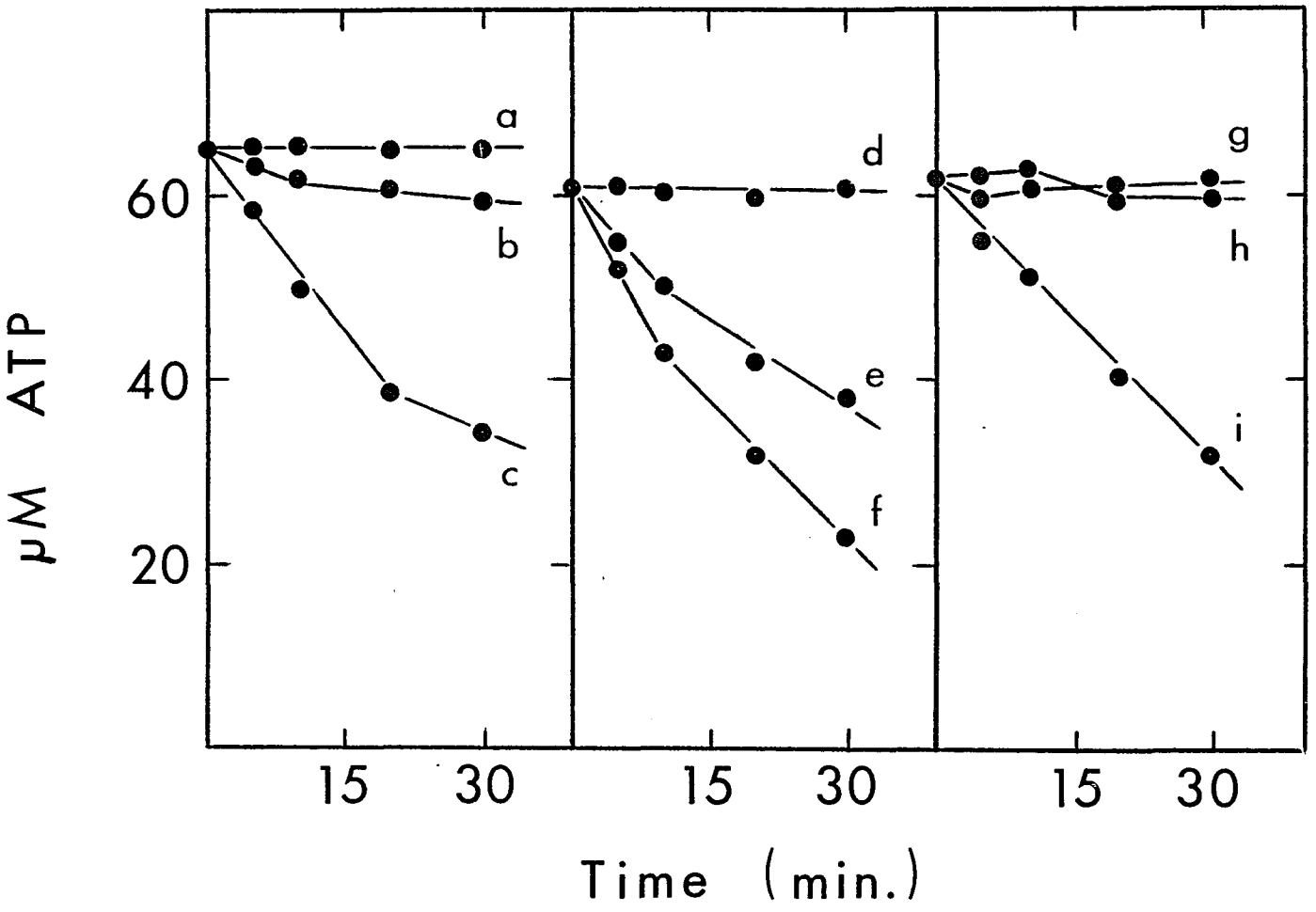
μM ATP
60
40
20
a
b
c
d
e
f
g
h
i
15
30
15
30
15
30
Time (min.)

Figure 25. Specific activity (in uM ADP formed/min/mg protein) plotted against pH for the ATPase activity of N_aPRTase in the presence of pyrophosphate but in the absence of both PRPP and nicotinate. The incubation mixtures contained 5 mM $MgCl_2$, 60 uM ATP and the following: (solid triangles) no more addition, (solid circles) 100 uM $Cr^{III}PP_i$ and (solid squares) 100 uM PP_i, in 50 mM Tris-phosphate buffer at pH 6-9 and 50 mM acetate containing 50 mM potassium phosphate at pH 5.0. The reaction was initiated and terminated as described under "Methods". Elution conditions: 5 ul sample injection volumes, 0.7 ml/min flow rate, 25 mM $(NH_4)_3PO_4$ pH 6.0 elution buffer, 25°C.

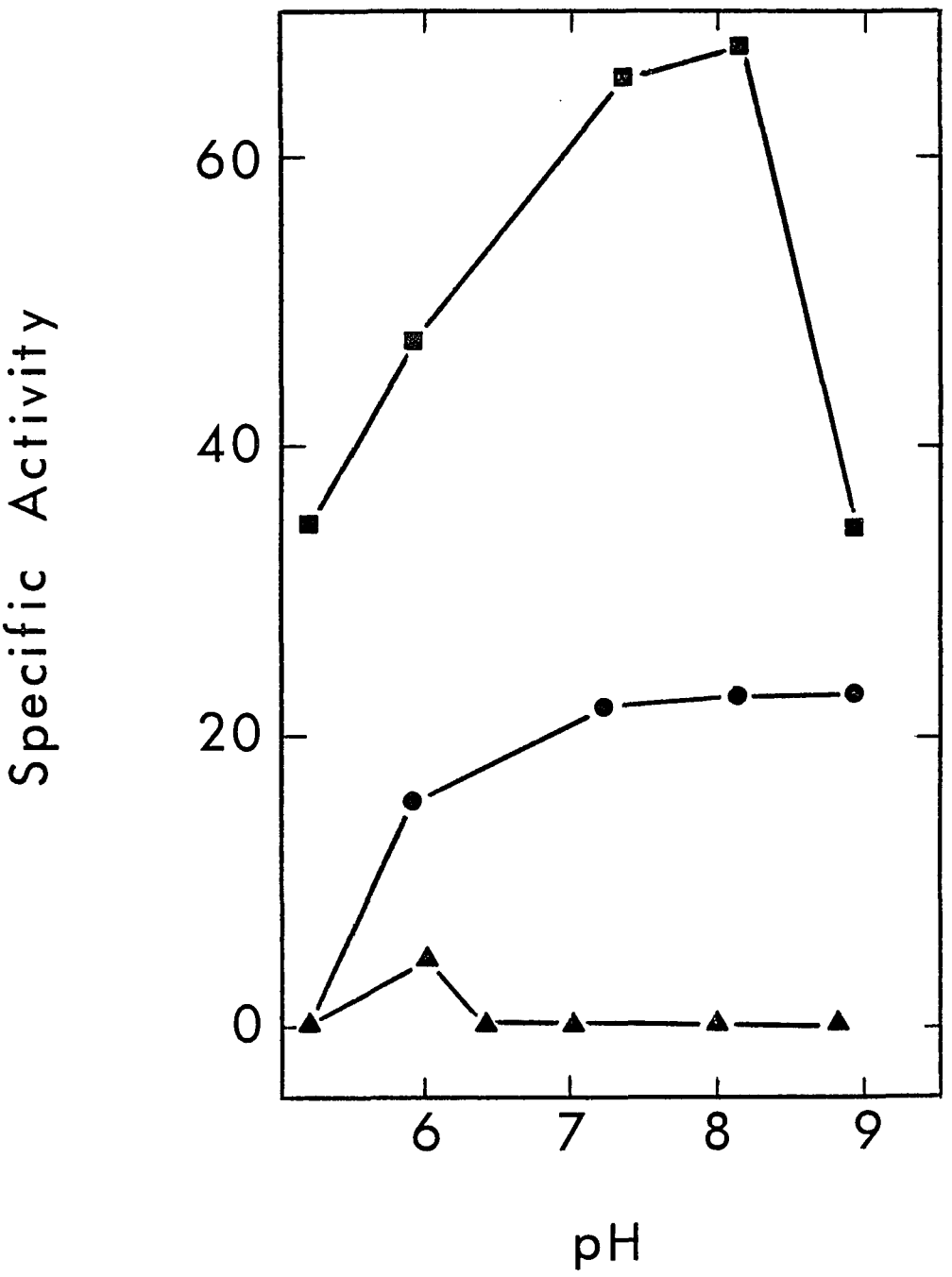
Specific Activity
60
40
20
0
6
7
8
9
pH

be provided by using substrate- and product-Cr^{III} complexes from which the metal ion does not dissociate readily.[62-64] Pilot studies of the effect of two such complexes on the N_aPRTase-catalyzed reaction, are presented here.

Double reciprocal plots of the initial velocity vs varied concentrations of nicotinate in the presence of different concentrations of Cr^{III}-pyrophosphate (and at constant and unsaturated concentration of PRPP and nicotinate) defined a parallel set of lines (uncompetitive inhibition). Independent studies of the inhibition by Mg-pyrophosphate at the same conditions were performed (Figures 26 and 27) and, as has been demonstrated before, a mixed-type inhibition by Mg-pyrophosphate was observed. Inhibition studies in the presence of both Cr^{III}-PP_i and Mg-PP_i gave rise to non-linear plots (Figures 26 and 27). This may indicate that Mg-PP_i and Cr^{III}-PP_i are not strictly competitive for site(s) on the enzyme.

Cr^{III}-PP_i has the capability to trigger the ATPase activity to a lesser extent (under the same conditions) as Mg-PP_i. A pH profile of the ATPase activity, determined in the presence of Cr^{III}-PP_i, is shown in Figure 25. Interestingly N_aPRTase shows a maximum ATPase activity between pH 6-9 when it is triggered by Cr^{III}-PP_i.

Double reciprocal plots of the initial velocity of N_aPRTase activity vs varied concentrations of ATP, at different concentration values of Cr^{III}ATP and at constant and unsaturated values of PRPP and nicotinate, is shown in Figure 28A. Cr^{III}ATP is shown to be a competitive inhibitor with K_i value approximately equal to 540 uM (Figure 28B). Thus these two compounds associate with N_aPRTase but do not serve as substrates.

Figure 26. Double reciprocal plots of the N_aPRTase initial velocity (v) vs the nicotinate concentrations in the presence of a) no inhibitor, b) 100 uM $Cr^{III}PP_i$, c) 100 uM PP_i and d) 100 uM $Cr^{III}PP_i$ and 100 uM PP_i together. Each data point represents (as determined by HPLC assay procedure) an average of the calculated rates of N_aMN and ATP concentration changes. The incubation solutions contained 5 mM $MgCl_2$, 50 uM ATP, 40 uM PRPP and varied concentrations of nicotinate (20, 40, 100 and 200 uM) in 50 mM Tris-phosphate buffer at pH 8.0. The reaction was initiated and terminated over a series of incubation times as described under "Methods". Elution conditions: 5 ul sample injection volumes, 0.7 ml/min flow rate, 25 mM $(NH_4)_3PO_4$ pH 6.0 elution buffer, 25°C.

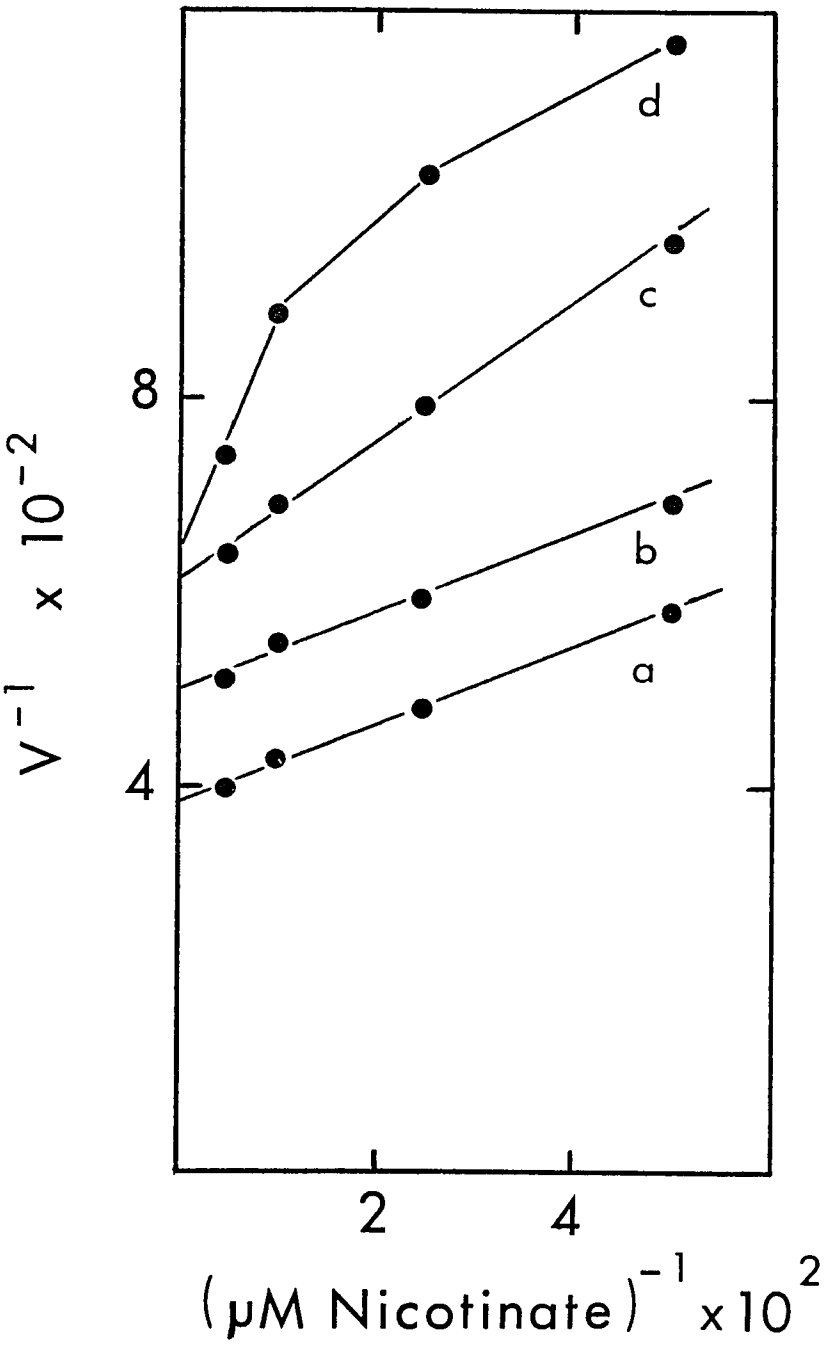
d
c
b
a
8
4
V^{-1} x 10^{-2}
2
4
(μM Nicotinate)$^{-1}$ x 10^{2}

Figure 27. Double reciprocal plots of the N_aPRTase initial velocity (v) vs the nicotinate concentrations in the presence of no inhibitor (—●—), 100 uM PP_i (—○—, 26A), 100 uM $Cr^{III}PP_i$ (—○—, 26B), 500 uM PP_i (—▲—, 26A), 500 uM $Cr^{III}PP_i$ (—▲—, 26B), 500 uM PP_i and 500 uM $Cr^{III}PP_i$ (—□—, 26A), and 100 uM PP_i and 100 uM $Cr^{III}PP_i$ (—□—, 26B). Each data point represents (as determined by HPLC assay procedure) an average of the calculated rates of N_aMN and ATP concentration changes. The incubation solutions contained 5 mM $MgCl_2$, 60 uM ATP, 40 uM PRPP and varied concentrations of nicotinate (20, 40, 100 and 200 uM) in 50 mM Tris-phosphate buffer at pH 8.0. The reaction was initiated and terminted over a series of incubation times as described under "Methods". Elution conditions: 5 ul sample injection volumes, 0.7 ml/min flow rate, 25 mM $(NH_4)_3PO_4$ pH 6.0 elution buffer, 25°C.

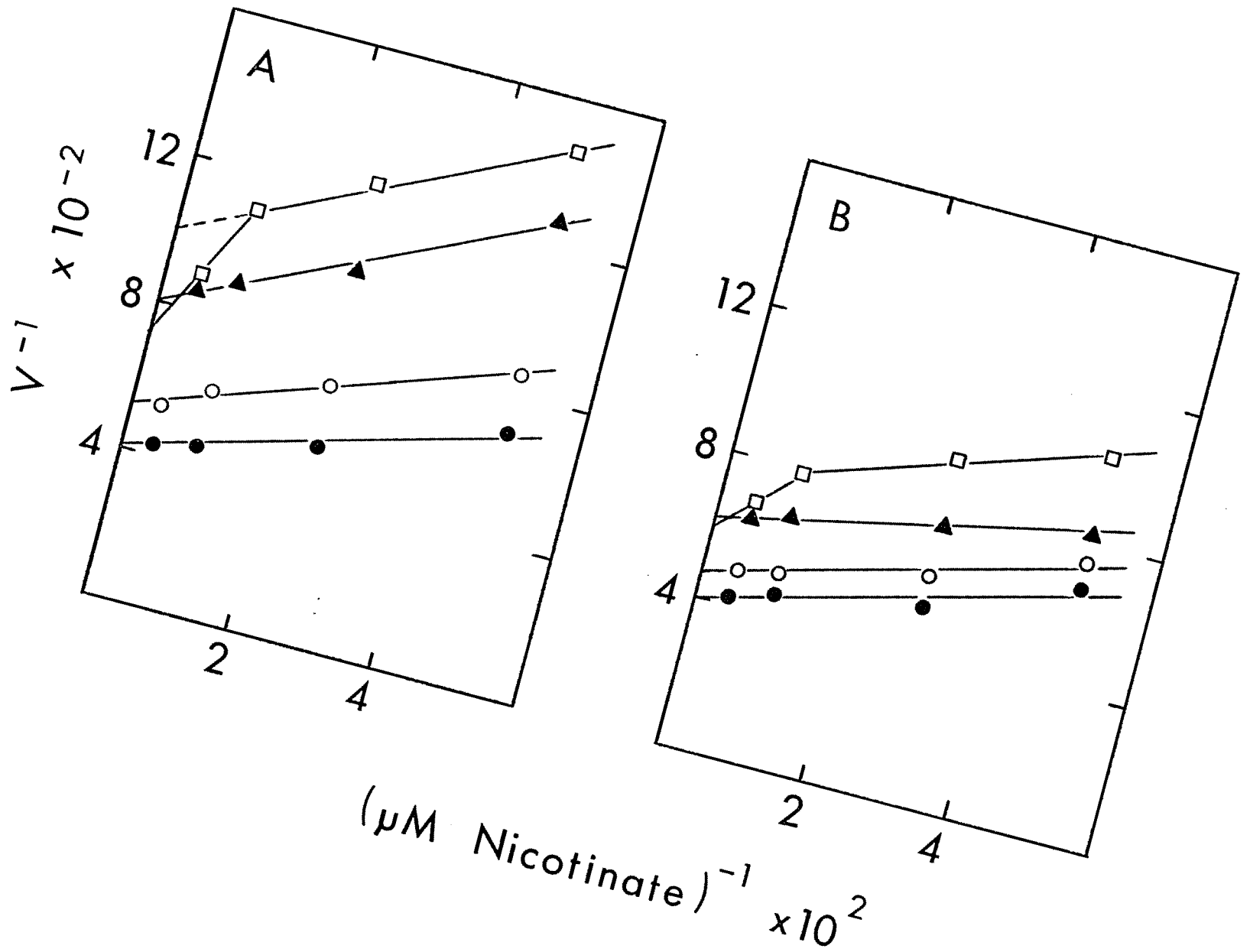
A
B
12
8
4
2
4
12
8
4
2
4
V⁻¹ x 10⁻²
(μM Nicotinate)⁻¹ x10²

Figure 28. A) Double reciprocal plots of the N_aPRTase initial velocity (v) vs the ATP concentrations in the presence of different concentration values of Cr^{III}ATP. Each data point represents (as determined by HPLC assay procedure) an average of the calculated rates of N_aMN and ATP concentration changes. Cr^{III}ATP concentrations, used in these experiments were 0 uM (a), 100 uM (b), 200 uM (c) and 400 uM (d). The incubation solutions contained 5 mM $MgCl_2$, 40 uM PRPP, 100 uM nicotinate and varied concentrations of ATP (30, 60, 120 and 240 uM) in 50 mM Tris-phosphate buffer at pH 8.0. The reaction was initiated and terminated over a series of incubation times as described under "Method". Elution conditions: 5 ul sample injection values, 0.7 ml/min flow rate, 25 mM $(NH_4)_3PO_4$ pH 6.0 elution buffer, 25°C. B) The replot of the $K_{m(app)}$ of A vs the Cr^{III}ATP concentrations.

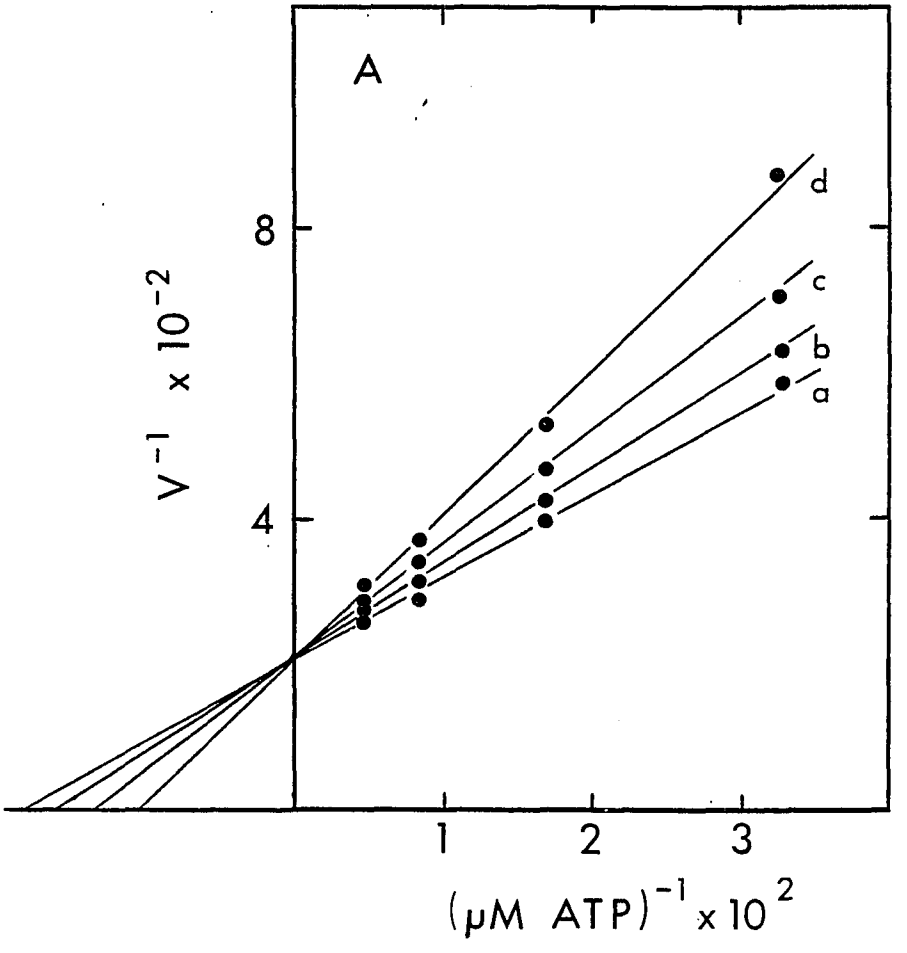
A
d
c
b
a
8
4
$V^{-1} \times 10^{-2}$
1
2
3
$(\mu M\ ATP)^{-1} \times 10^{2}$

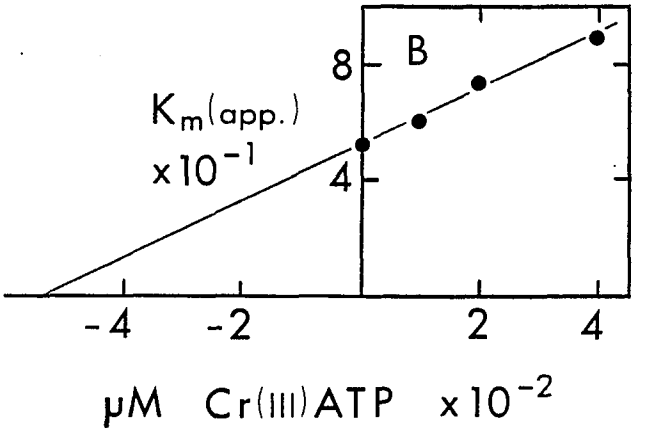
B
8
4
$K_m(app.)$
$\times 10^{-1}$
-4
-2
2
4
$\mu M\ Cr(III)ATP \times 10^{-2}$

Binding Studies with Flow Dialysis

Elution profiles of the labelled nicotinate are illustrated in Figure 29. In these experiments, it was observed that nicotinate does not bind to the phosphorylated-N_aPRTase, whereas in the presence of the phosphorylated-N_aPRTase and PRPP, nicotinate bound tightly to the enzyme. Such experiments strongly suggest that PRPP must bind to the phosphorylated enzyme before nicotinate can bind. Moreover, a second study showed that nicotinate may associate with the unphosphorylated enzyme, in an unspecified manner. However, from other studies conducted and previous studies by Kosaka et al.,[24,25] this binding may be considered to be a non-productive binding from a kinetic point of view.

Calculation of Kinetic Constants

As shown by Segel[68] the initial velocity equation for bi uni uni uni ping-pong ter bi system is represented by equation 1.

$$\frac{v}{V_{max}} = \frac{[A][B][C]}{K_{ia} K_{m_B}[C] + K_{m_C}[A][B] + K_{m_B}[A][C] + K_{m_A}[B][C] + [A][B][C]} \quad (1)$$

This system and equation can be used to calculate kinetic constants for the N_aPRTase catalyzed reaction if the following adjustments are made. As shown in equation 2, the Cleland notation for the above described system also describes N_aPRTase system if we begin the sequence at substrate C.

Figure 29. Flow dialysis study with C^{14}-nicotinate. The incubation mixtures in the upper chamber is as follows: 5 mM $MgCl_2$ and 1 mM ATP (—O—), 5 mM $MgCl_2$, 1 mM ATP and 20 uM N_aPRTase (—●—), 5 mM $MgCl_2$ and 20 uM N_aPRTase (—△—) and 5 mM $MgCl_2$, 1 mM ATP, 0.5 mM PRPP and 20 uM N_aPRTase (—▲—). After 1 minutes 40 uM 7-[C^{14}]-nicotinate acid (0.1 uCi) was added to the upper chamber. The time and the amount of added unlabelled nicotinic acid is indicated on the graph. The lower chamber buffer is 50 mM potassium phosphate containing 5 mM $MgCl_2$, flow rate is 3 ml/minute/fraction, 25°C.

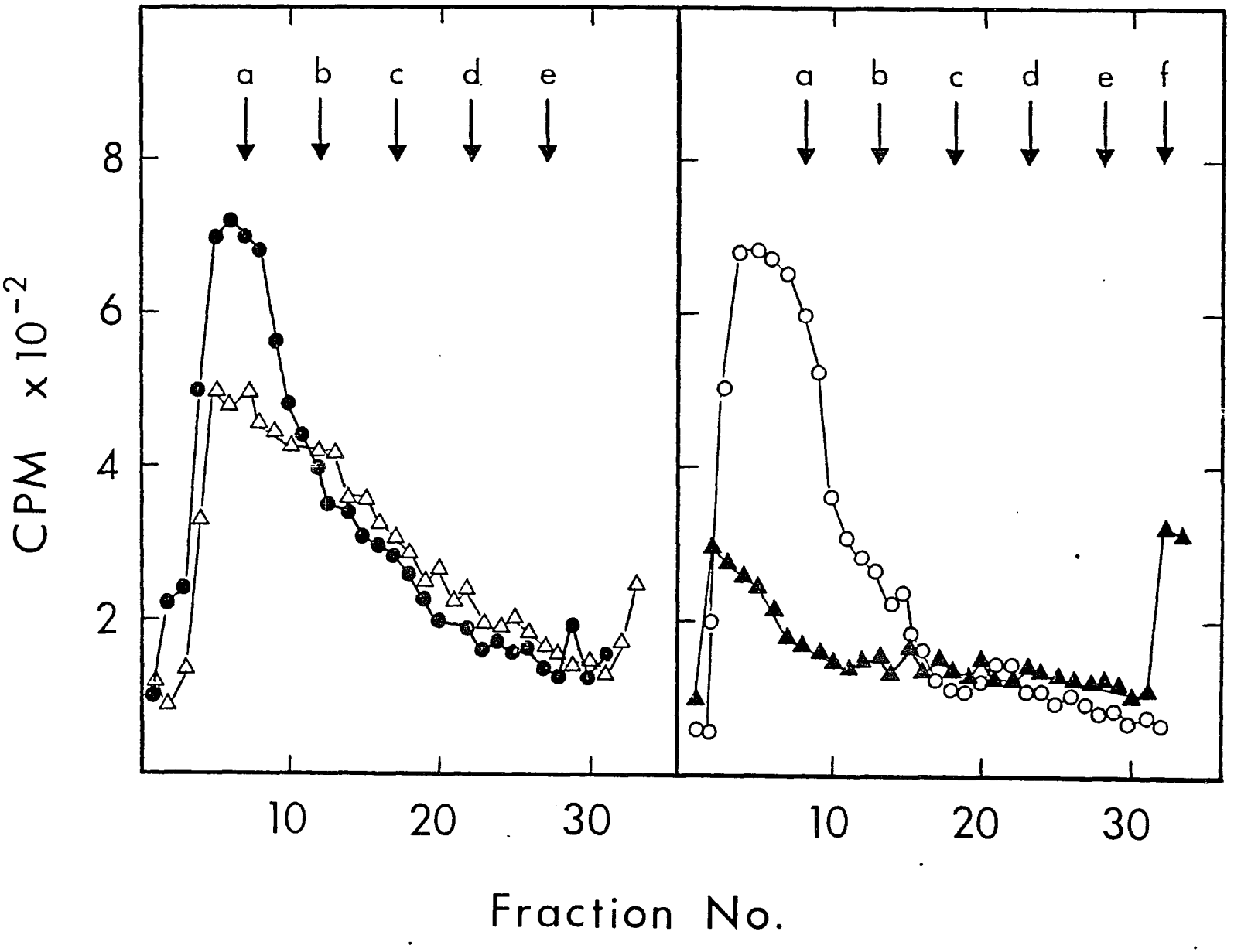
a
b
c
d
e
f
8
6
4
2
CPM x 10⁻²
10
20
30
Fraction No.

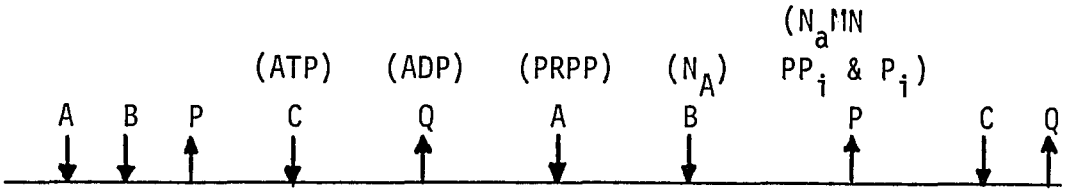

(2)

Thus equation 1 can be represented by equation 3 and from reciprocal rearrangements of this equation (equation 4 provides one such example) the appropriate kinetic constants can be calculated using the data shown in Figures 15-17.

$$\frac{v}{V_{max}} = \frac{[PRPP][N_A][ATP]}{K_{i_{PRPP}} K_{m_{N_A}} [ATP] + K_{m_{ATP}} [PRPP][N_A] + K_{m_{N_A}} [ATP][PRPP]} \qquad (3)$$
$$+ K_{m_{PRPP}} [ATP][N_A] + [PRPP][N_A][ATP]$$

$$\frac{1}{v} = \frac{K_{m_{PRPP}}}{V_{max}} \left[1 + \frac{K_{i_{PRPP}} K_{m_{N_A}}}{K_{m_{PRPP}} \times 0.67[ATP]} \right] \frac{1}{[PRPP]} \qquad (4)$$
$$+ \frac{1}{V_{max}} \left[1 + \frac{K_{m_{N_A}}}{0.67[ATP]} + \frac{K_{m_{ATP}}}{[ATP]} \right]$$

These constants are represented in Table 7. As shown in Table 7, the value of K_m of ATP is approximately 4 times those of nicotinate and PRPP which are approximately equal. Also the value of K_i for PRPP is one-fourth the K_m for this substrate.

Table 7. Kinetic constants for N_aPRTase.

Kinetic Constant	Value
V_{max}	2.5±.4 x 10^{-2} umol N_aMN/min
$K_{m(ATP)}$	70 ± 10 uM
$K_{m(PRPP)}$	24 ± 3 uM
$K_{m(nicotinate)}$	23 ± 4 uM
$K_{i(PRPP)}$	5 ± 1 uM

DISCUSSION

In order to study any enzyme, a sensitive and reliable assay must be developed. Spectrophotometers provide an excellent tool for monitoring enzyme catalyzed reaction whenever one of the substrates or the products has an absorption maximum at specific wavelength whereas the other substrates and products do not. NADH dependent dehydrogenases are ideal examples of such a group of enzymes.[70] Indirect spectrophotometric assay procedures also have been designed where a second enzyme, which either produces one of the substrate or utilizes one of the products and which can be monitored spectrophotometrically, is added to the assay mixture for the desired enzyme. Commercially available (Sigma Chemical) mixtures of Pyruvate Kinase and Lactate Dehydrogenase provide an example of such procedures. However, indirect assay procedures may give rise to a number of complications, especially in kinetic studies. In the past few decades, the utilization of radioactive isotopes has become a very useful tool to assay for many enzymes for which a spectrophotometric assay is not possible. During this type of procedure, a radioactive substrate is incubated with the enzyme in the assay mixture to form a radioactive product, then through the use of chromatographic methods the product is separated from the substrate and identified. These procedures provide the sensitivity required for kinetic analysis but they are time consuming. Recently, because of rising costs and waste disposal problems (and because of the hazards involved), scientists have searched for alternative methods. HPLC lends itself as an excellent tool for rapid separation and identification of specific substrates and

products. It also provides the sensitivity and reliability required for kinetic studies to be accomplished. The most interesting aspect of such a method, is that one can observe the utilization and the formation of most of the substrates and products at the same time.

In this thesis I describe the development of an HPLC assay method to monitor the enzymatic activity of nicotinate phosphoribosyltransferase, in which I was successful in separating two substrates and two products of the reaction, namely ATP, nicotinate, ADP and N_aMN and in identifying them spectrophotometrically at 254 nm. I also established a direct relationship between the concentrations of the injected substrate and product solutions and the peak areas and peak heights of the resulting elution profile. Peak height measurements and these standard curves were used to calculated the concentration of each reactant during the time course of the reaction. This new method allows a sensitive and reliable quantitative measurement of the nicotinate phosphoribosyltransferase in a short time without the use of radioactive materials.

Moreover, a purification procedure which can provide an adequate amount of highly purified enzyme is essential. Kosaka et al. first developed a purification procedure for N_aPRTase from yeast,[24] and then modified this procedure[25] by making use of affinity chromatography. Although this procedure provided highly purified enzyme with a high specific activity, their method is lengthy and gave a very poor yield (0.3 mg 16 lbs of yeast). Since thorough kinetic studies, binding studies and (later on in this laboratory) studies of the active site geometry by NMR spectroscopy were planned, a purification procedure

with better yield became essential. I have succesfully developed a procedure which yielded a highly purified protein with specific activity equal or slightly higher than that of Kosaka et al.[25] when the same assay conditions were utilized. Most important, however, this procedure provides very good yield of enzyme (10 mg/6 lbs of yeast). Moreover, this procedure enabled us to obtain another enzyme OPRTase from the same yeast preparation.

In order to elucidate the kinetic mechanism of N_aPRTase, Kosaka et al.[24,25] have represented convincing evidence for the formation of a phosphorylated-N_aPRTase when incubated in the presence of ATP and Mg^{2+} and in the absence of the other substrates. They have been able to isolate the enzyme intermediate and demonstrate that the inorganic phosphate did not disassociate from the enzyme except when all other substrates are present. However, the double-reciprocal initial velocity plots and the selective product inhibition studies they performed suggested that ADP may not leave the enzyme except after the addition of the other two substrates. These results are uninterpretable because of the demonstration of substrate inhibition caused by high concentrations of PRPP (Figure 11). The concentrations of PRPP utilized in their experiments[25] were in the region of this profound inhibition. Employing the HPLC assay, double reciprocal initial velocity patterns have suggested a ping-pong step involved in the ATP addition to the enzyme. However, these studies do not distinguish the order of addition of the other two substrates. The lack of any exchange between $[^{32}P]$-PP_i/PRPP whereas a slow exchange between $[^{14}C]$-N_A/N_aMN only in the presence of ATP may suggest that PRPP must

add before nicotinic acid and that the inorganic phosphate leaves after N_aMN. However, stronger evidence for this interpretation came from studies of the ATPase activity of the enzyme, triggered by either products PP_i or N_aMN. The fact that PRPP, and not nicotinate, inhibits the hydrolysis of ATP in the presence of either PP_i or N_aMN indicates that PRPP may bind to the phosphorylated enzyme with a higher affinity than either PP_i or N_aMN preventing these products from binding. On the other hand, because nicotinate could not bind to the phosphorylated enzyme either of the two products, PP_i or N_aMN, were able to bind to the phosphorylated enzyme and cause the release of the phosphate group. In addition these results provide evidence that PP_i also has to dissociate from $N_aPRTase$ before the phosphate group, and that PP_i and N_aMN may dissociate from the enzyme at random. Supportive evidence for the order of addition of PRPP and nicotinate came from binding studies in which we demonstrated that nicotinate failed to bind to the phosphorylated enzyme. Whereas in the presence of PRPP, nicotinate bound tightly to the phosphorylated enzyme. Product inhibition studies conducted with PP_i (either the second or third product released) support the random release of the second and third products (PP_i and N_aMN).

Figure 30 represents, in the Cleland nomenclature, the proposed kinetic mechanism for $N_aPRTase$ activity. This is a Uni Uni Bi Ter Ter Quad system in which the second and third products can leave at random. Also represented in Figure 30 is the enzyme catalyzed ATPase activity (dotted lines) promoted by PP_i and N_aMN.

In order to determine the role of metal ions in the action of

N_aPRTase, we have initiated inhibition studies by Cr^{III} complexes of ATP and PP_i. The competitive inhibition of MgATP function by Cr^{III}-ATP may suggest that metal-bound ATP is the actual substrate for N_aPRTase, whereas the non-linear inhibition by Cr^{III}-PP_i in the presence of Mg-PP_i indicates that these complexes are not strictly competitive inhibitors of the N_aPRTase forward reaction. Although these studies by themselves are not conclusive, they set the stage for the NMR studies of the active site geometery for the N_aPRTase. Clearly, knowledge of the kinetic mechanism of the N_aPRTase reaction and the design of new and better assay and purification procedures for N_aPRTase, facilitate further studies of this enzyme-catalyzed reaction.

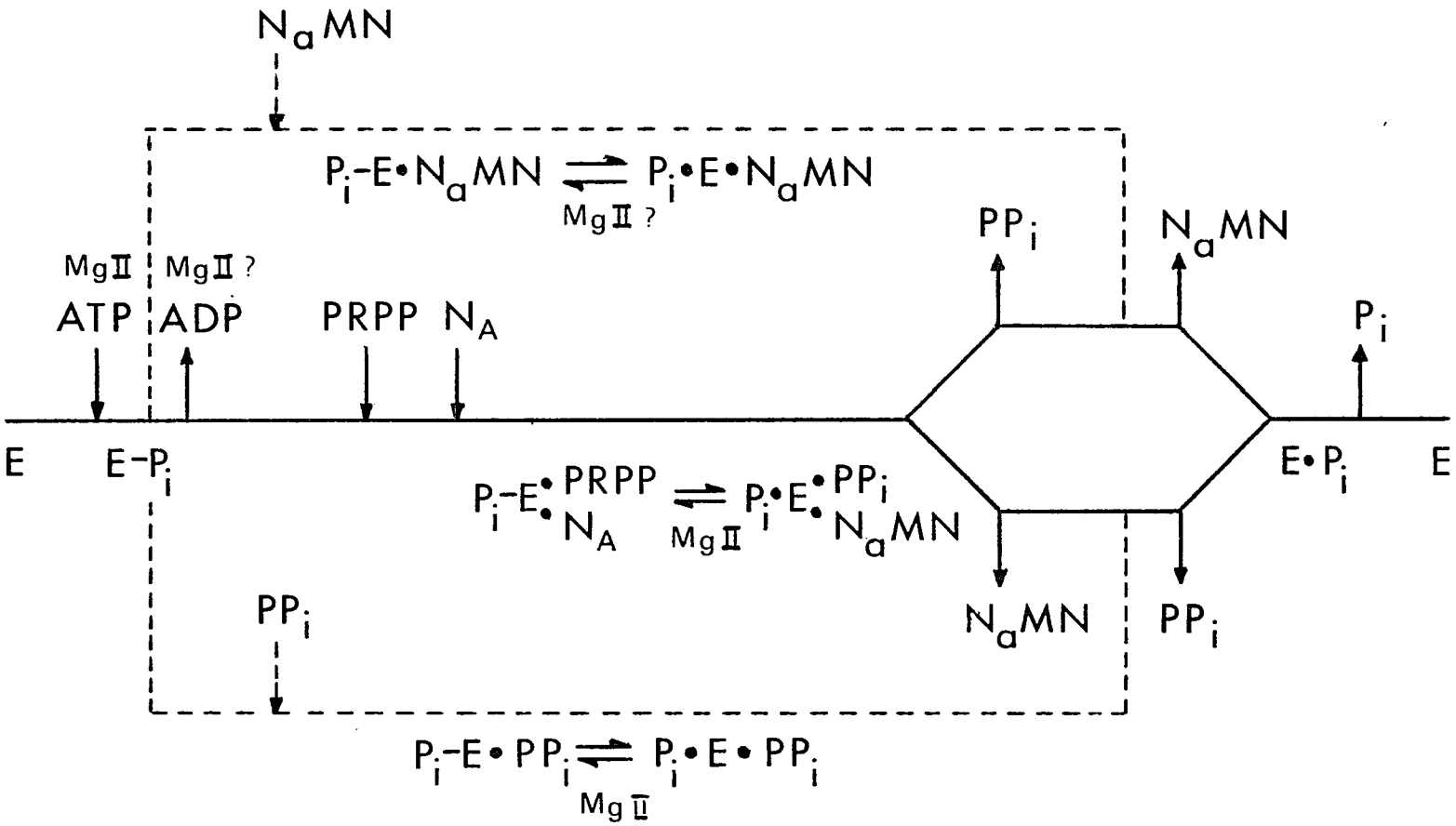

Figure 30. The Cleland nomenclature for the proposed Uni Uni Bi Ter Ter Quad kinetic mechanism for N_aPRTase enzyme, in which the second and third substrates can dissociate in random. Dotted lines represent the N_aPRTase-catalyzed ATPase activity.

REFERENCES

(1) Nakamura, S., Ikeda, M., Tshji, H., Nishizuka, Y., and Hayaishi, O. (1963) Biochem. Biophys. Res. Comm. 13, 285-290.

(2) Preiss, J. and Handler, P. (1958) J. Biol. Chem. 233, 488-492.

(3) Preiss, J. and Handler, P. (1958) J. Biol. Chem. 233, 493-500.

(4) Imsande, J. (1961) J. Biol. Chem. 236, 1494-1497.

(5) Kornberg, A. (1950) J. Biol. Chem. 182, 779-793.

(6) Lin, L. F. H., Lan, S. J., Richardson, A. H. and Henderson, L. M. (1972) J. Biol. Chem. 247, 8016-8022.

(7) Kuwahara, M. and Chaykin, S. (1973) J. Biol. Chem. 248, 5095-5099.

(8) Andreoli, A. J., Ikeda, M., Nishizuka, Y., and Hayaishi, O. (1963) Biochem. Biophys. Res. Comm. 12, 92-97.

(9) Imai, T. (1973) J. Biochem. (Tokyo) 73, 139-153.

(10) Gholson, R. K., Ueda, I., Ogasuwora, N., and Henderson, L. M. (1964) J. Biol. Chem. 239, 1208-1214.

(11) Iwai, K. and Toguchi, H. (1974) Biochem. Biophys. Res. Comm. 56, 884-891.

(12) Mann, D. F. and Byerrum, R. U. (1974) J. Biol. Chem. 249, 6817-6823.

(13) Taguchi, H. and Iwai, K. (1974) J. Nutr. Sci. Vitaminol. 20, 269-281.

(14) Packman, P. M. and Jakoby, W. B. (1965) J. Biol. Chem. 240 PC 4107-4108.

(15) Iwai, K., Shibata, K., Taguchi, H., and Itakura, T. (1979) Agric. Biol. Chem. 43, 345-350.

(16) McLaren, J., Domingo, T. C. N., and Olivera, B. M. (1973) J. Biol. Chem. 248, 5144-5159

(17) Koshland, D. E., Jr., "The Enzymes" (3rd Ed.), P. Boyer (Ed.) vol. 1, Academic Press, New York (1970) p. 341.

(18) Jones, O. W., Ashton, D. M., and Wyngaarden, J. B. (1962) J. Clin. Invest. 41, 1805-1815.

(19) Kelley, W. N and Wyngaarden, J. B. (1974) Adv. Enzymol. 41, 1-33.

(20) Lesch, M. and Nyhan, W. L. (1964) Amer. J. Med. 36, 561-570.

(21) Smith, L. H., Jr., Huguley, C. M., Jr., and Bain, J. A., in "The Metabolic Basis of Inherited Diseases" (3rd Ed.), Stanbury, J. B., Wyngaarden, J. B., and Fredrickson, D. S. (Ed.) McGraw-Hill, New York (1972) p. 1003.

(22) Gershon, S. L. and Fox, I. H. (1974) J. Lab. Clin. Med. 84, 179-186.

(23) Smith, L. D. and Gholson, R. K. (1969) J. Biol. Chem. 244, 68-71.

(24) Kosaka, A., Spivey, H. O., and Gholson, R. K. (1971) J. Biol. Chem. 246, 3277-3282.

(25) Kosaka, A., Spivey, H. O., and Gholson, R. K. (1977) Arch. of Biochem. and Biophys. 179, 334-341.

(26) Imsande, J. (1964) Biochim. Biophys. Acta 85, 255-264.

(27) Niedel, J. and Dietrich, L. S. (1973) J. Biol. Chem. 248, 3500-3505.

(28) Seifert, R., Kittler, M., and Hilz, H., in "Current Aspects of Biochemical Energetics", Kaplan, N. O. and Kennedy, E. P. (Ed.) Academic Press, New York (1966) p. 413.

(29) Kahn, V. and Blum, J. J. (1967) Biochim. Biophys. Acta 146, 305-308.

(30) Shibata, K. and Iwai, K. (1980) Agric. Biol. Chem. 44, 293-300.

(31) Iwai, K., Shibata, K., and Taguchi, H. (1979) Agric. Biol. Chem. 43, 351-355.

(32) Shibata, K. and Iwai, K. (1980) Agric. Biol. Chem. 44, 287-292.

(33) Shibata, K. and Iwai, K. (1980) Biochim. Biophys. Acta 611, 280-288.

(34) Shibata, K. and Iwai, K. (1980) Agric. Biol. Chem. 44, 119-123.

(35) Ismande, J., and Handler, P., in P. D. Boyer (ed.) "The Enzymes", Vol. 5, 2nd Ed., Academic Press, New York, p. 281.

(36) Giacomello, A. and Salerno, C. (1978) J. Biol. Chem. 253, 6038-6044.

(37) Henderson, J. F., Brox, L. W., Kelley, W. N., Rosenbloom, F. M. and Seegmiller, J. E. (1968) J. Biol. Chem. 243, 2514-2522.

(38) Krenitsky, T. A. and Papaioannou, R. (1969) J. Biol. Chem. 244, 1271-1277.

(39) Victor, J., Greenberg, L. B. and Sloan, D. L. (1979) J. Biol. Chem. 254, 2647-2655.

(40) Chelsky, D. and Parson, S. M. (1975) J. Biol. Chem. 250, 5669-5673.

(41) Brashear, W. T. and Parsons, S. M. (1975) J. Biol. Chem. 250, 6885-6890.

(42) Morton, D. P. and Parsons, S. M. (1976) Arch. Biochem. Biophys. 175, 677-686.

(43) Kleeman, J. E. and Parsons, S. M. (1976) Arch. Biochem. Biophys. 175, 687-693.

(44) Bell, R. M. and Koshland, D. S. (1970) Biochem. Biophys. Res. Comm. 38, 539-545.

(45) Spector, L. B. (1980) Proc. Nat. Acad. Sci (U.S.) 77, 2626-2630.

(46) Kaneti, J., Golorinsky, E., Yukhovsky, I., and Genechev, D. (1970) J. Theor. Biol. 26, 19-27.

(47) Goitein, R. K., Chelsky, D., and Parsons, S. M. (1978) J. Biol. Chem. 253, 2963-2971.

(48) Victor, J., Leo-Mensah, A., and Sloan, D. L. (1979) Biochemistry 18, 3597-3603.

(49) Sloan, D. L., Ali, L. Z., Hanna, L., Raynie, K. C., and Strauss, R. S. (1981) in "Intact Human Cell Lines in Studies of Inborn Metabolic Diseases", NIAMDD Monograph (in press).

(50) Ali, L. Z., and Sloan, D. L. (1981) J. Biol. Chem. 256 (in press).

(51) Hanna, L., Ali, L. Z., and Sloan, D. L. (1979) Biophys. J. 25, 162a, abstract.

(52) Hanna, L. and Sloan, D. L. (1980) Analytical Biochem. 103, 230-234.

(53) Umezu, K., Amaya, T., Yashismoto, A., and Tomita, K. (1971) J. Biochem. (Tokyo) 70, 249-262.

(54) Davis, B. J. (1964) Ann. N.Y. Acad. Sci. 121, 404-427.

(55) Weber, K. and Osborn, M. (1969) J. Biol. Chem. 244, 4406-4412.

(56) Shapiro, A. L., Vinuela, E., and Maizel, J. V. (1967) Biochem. Biophys. Res. Comm. 28, 815-820.

(57) Wrigley, C. W. (1971) Methods Enzymol. 22, 559-564.

(58) Righetti, P. G. and Drysdale, J. W. (1974) J. Chromatography 98, 271-321.

(59) Lowry, O. H., Rosebrough, N. J. Farr, L., and Randall, R. J. (1951) J. Biol. Chem. 193, 265-275.

(60) Kornberg, A. (1950) J. Biol. Chem. 182, 779-793.

(61) Brown, A. N (1946) Arch. Biochem. 11, 269-278.

(62) Janson, C. A. and Cleland, W. W. (1974) J. Biol. Chem. 249, 2572-2574.

(63) Dunaway-Mariano, D. and Cleland, W. W. (1980) Biochemistry 19, 1496-1505.

(64) Cleland, W. W. and Mildvan, A. S. in "Advances in Inorganic Biochemistry" vol 1, Eichhorn, G. L. and Marzilli, L. G. (Ed.) Elsevier/North-Holland, New York (1979) p. 180-183.

(65) Postmas, C. and King, E. (1955) J. Phys. Chem. 59, 1208-1216.

(66) Chen, P. S., Jr., Toribara, T. Y., and Warner, H. (1956) Analytical Chemistry 28, 1756-1758.

(67) Ames, B. N and Dublin, D. T. (1960) J. Biol. Chem. 235, 769-775.

(68) Segel, I. H., in "Enzyme Kinetics - Behavior and Analysis of Rapid Equilibrium and Steady-state Enzyme Systems", A. Wiley-Interscience Publication (1975) p. 684-735.

(69) Colowick, S. P. and Womack, F. C. (1969) J. Biol. Chem. 244, 744-777.

(70) Sloan, D. L. and Velick, S. F. (1973) J. Biol. Chem. 248, 5419-5423.

CURRICULUM VITAE

NAME: Lewis S. Hanna

ADDRESS: 125-10 Queens Blvd., Apt. 621, Kew Gardens, N.Y. 11415

TELEPHONE NO.: (212) 793-0819

BIRTHDATE: April 28, 1946

CITIZENSHIP: U.S.A.

EDUCATION:

Undergradute: B.S., Chemistry and Physics, Cairo University, Cairo, Egypt, 1968

Graduate: Ph.D., Biochemistry, City University of N.Y., 1981

TEACHING EXPERIENCE: Teaching Fellowship - City College of N.Y. 1976-1980

ACADEMIC HONORS: Sigma Xi, 1980

PROFESSIONAL SOCIETIES:

American Association for the Advancement of Science, 1980-present

American Chemical Society, 1980-present

Biophysical Society, 1980-present

New York Academy of Science, 1980-present

PUBLICATIONS:

1) L. S. Hanna, L. Ali and D. L. Sloan "High Pressure Liquid Chromatography Procedures for Detecting Nicotinate- and Hypoxanthine/Guanine Phosphoribosyltransferase Activities." Biophys. J. 25, A 162 (1979), Abstract.

2) L. S. Hanna and D. L. Sloan, "A High-Pressure Liquid Chromatography Procedure for Monitoring Nicotinate Phosphoribosyltransferase Activity." Anal. Biochem. 103, 230-234 (1980).